

Signature Kernel Conditional Independence Tests in Causal Discovery for Stochastic Processes

Georg Manten^{†,1,2,3}, Cecilia Casolo^{†,1,2,3}, Emilio Ferrucci⁴, Søren Wengel Mogensen⁵,
Cristopher Salvi⁶, Niki Kilbertus^{1,2,3}

¹Technical University of Munich

²Helmholtz Munich

³Munich Center for Machine Learning

⁴Mathematical Institute, University of Oxford

⁵Department of Automatic Control, Lund University

⁶Department of Mathematics, Imperial College London

[†]equal contribution

Abstract

Inferring the causal structure underlying stochastic dynamical systems from observational data holds great promise in domains ranging from science and health to finance. Such processes can often be accurately modeled via stochastic differential equations (SDEs), which naturally imply causal relationships via ‘which variables enter the differential of which other variables’. In this paper, we develop a kernel-based test of conditional independence (CI) on ‘path-space’—solutions to SDEs—by leveraging recent advances in signature kernels. We demonstrate strictly superior performance of our proposed CI test compared to existing approaches on path-space. Then, we develop constraint-based causal discovery algorithms for acyclic stochastic dynamical systems (allowing for loops) that leverage temporal information to recover the entire directed graph. Assuming faithfulness and a CI oracle, our algorithm is sound and complete. We empirically verify that our developed CI test in conjunction with the causal discovery algorithm reliably outperforms baselines across a range of settings.

1 Introduction

Understanding cause-effect relationships from observational data can help identify causal drivers for disease progression in longitudinal data and aid the development of new treatments, understand the underlying influences of stock prices to support lucrative trading strategies, or speed up scientific discovery by uncovering interactions in complex biological or chemical systems such as gene regulatory pathways.

Causal discovery (or causal structure learning) has received continued attention from the scientific community for at least two decades (Glymour et al., 2019, Spirtes et al., 2000, Vowels et al., 2022) with a notable uptick in previous years particularly regarding differentiable score-based causal discovery (Annadani et al., 2023, Brouillard et al., 2020, Charpentier et al., 2022, Hägele et al., 2023, Lorch et al., 2021, Zheng et al., 2018, 2020), score matching (Montagna et al., 2023a,b, Rolland et al., 2022), and other deep-learning based approaches (Chen et al., 2022, Ke et al., 2020, 2023, Yu et al., 2019). Many of these approaches aim at improving the scalability of causal discovery in the number of variables and observations as well as at incorporating uncertainty or efficiently making use of interventional data.

However, causal discovery from time series data has received much less attention in general and been mostly neglected in particular in these recent advances. At a fundamental level, causal effects can only ‘point into the future’, and it may seem that time resolved data should

make causal discovery simpler. However, except for simple cases, this is not necessarily true (Lawrence et al., 2021, Runge et al., 2023, 2019, Singer, 1992) as dynamical systems may exhibit temporally changing causal dependencies as well as confounding introduced by discrepancies in the intrinsic dynamical timescales and the sampling frequency. The bulk of existing work assumes observations to be sampled on a regular time grid with a discrete (auto-regressive) law for how past observations $(X_{t-\tau}, \dots, X_{t-1})$ determine the present $X_t = f(X_{t-\tau}, \dots, X_{t-1}, \varepsilon_t)$ for some time lag $\tau \in \mathbb{N}$ and a fixed function f (Assaad et al., 2022, Hasan et al., 2023). Overcoming the fundamental limitations imposed by this ‘discrete-time’ assumption is a major challenge (Runge et al., 2019), which we tackle in this work.

Data generating process. We assume observational data to follow a stochastic process $X := (X^1, \dots, X^d)$, with X^k taking values in \mathbb{R}^{n_k} ($n_k \geq 1$), and X satisfying the following system of path-dependent SDEs

$$\begin{cases} dX_t^k = \mu^k(X_{[0,t]})dt + \sigma^k(X_{[0,t]})dW_t^k, \\ X_0^k = x_0^k \quad \text{for } k \in [d] := \{1, \dots, d\}. \end{cases} \quad (1)$$

We call this the *SDE model*; a very similar model, the *stochastic causal kinetic model*, was recently introduced in Peters et al. (2022). The subscript $[0, t]$ at X means that μ^k (the ‘drift’) and σ^k (the ‘diffusion’) are functions of the entire solution up to time t , i.e., they are defined on $C([0, +\infty), \mathbb{R}^n)$ (or some suitable subspace thereof), where $n := n_1 + \dots + n_k$. Each W^k is an m_k -dimensional Brownian motion, and σ^k maps to $n_k \times m_k$ -dimensional matrices. The noises W^k together with the (possibly random) initial conditions x_0^k are jointly independent.¹ Hence, the SDE together with a distribution over initial conditions defines our assumed ground truth *data generating process*. Individual observations are paths, which in practice translate to stochastic, potentially irregularly sampled time-series observations for $X_{[0, T]}^k$ with a maximum observation time T , see Figure 1. The choice not to make the coefficients explicitly time-dependent is deliberate and motivated by the requirement of *causal stationary* (the causal relations between variables do not change over time).

Induced causal graph. Eq. (1) naturally implies cause-effect relationships: we call $i \in [d]$ a parent of $j \in [d]$ ($i \in \text{pa}_j$) when either μ^j or σ^j is not constant in the i -th argument. These parental relationships define a directed graph $\mathcal{G} = (V, E)$ which we also call *dependency graph* of the SDE model. The **goal of causal discovery** is then to infer the \mathcal{G} induced by the SDE model from a sample of observed solution paths, depicted in Figure 1. Here, we only consider data generating processes leading to directed graphs without cycles of length greater than one (i.e., only loops $X^k \rightarrow X^k$ are allowed). We will still call these directed acyclic graphs (DAGs) for simplicity. The additional challenges arising from dropping the acyclicity assumption is discussed in Appendix E as an interesting direction for future work. Moreover, we assume all relevant variables X to be observed. When only partial observations are available, i.e., some processes are unobserved, any constraint-based algorithm based on asymmetric *local independence* requires exponentially many oracle calls (Mogensen, 2023, Mogensen and Hansen, 2022). The partially observed case is therefore challenging in the local independence framework, however, the symmetric conditional independence framework we describe may be extended directly to the partially observed setting.

Despite these limitations, eq. (1) goes far beyond common assumptions in causal discovery from time-series data, also in comparison with similar models as in Peters et al. (2022): (a) It does not rely on the ‘discrete-time’ assumption (neither in the underlying model nor the actual observations). (b) Path-dependence (μ^k, σ^k may depend on the entire previous history $X_{[0, t]}$ of paths), including delayed SDEs, is typically not captured in existing approaches. (c) It goes beyond ‘additive observation noise’ as it incorporates ‘driving noise’ where causal

¹See Rogers and Williams (2000) for details, Evans (2006) for a concise introduction, and Appendix A.1 for more intuition.

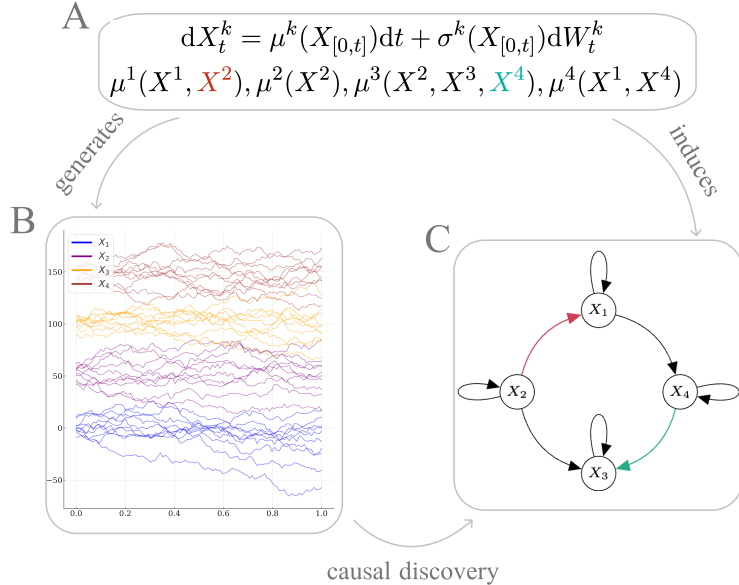


Figure 1: Overview of causal discovery in our setting. The data generating mechanism (A) generates samples (B) and induces a causal graph (C). The goal of constraint-based causal discovery is to use conditional independence relations on the observed trajectories (B) to determine the causal graph (C).

dependence may also come from the diffusion, which cannot be captured by the mean of observed paths.

Contributions. We develop sound and complete constraint-based algorithms for (a) inferring the full DAG, (b) inferring the completed partially directed acyclic graph (CPDAG) representing the Markov equivalence class from path-valued observations (assuming a conditional independence test oracle and faithfulness). While (a) yields strictly stronger results, it relies on a different independence model. To render these algorithms applicable, we also propose flexible CI tests on path-space building on recent advances in signature kernels. After extensive empirical evaluations, demonstrating the superior performance of our CI tests (for different types of CI models), we combine our test with the causal discovery algorithms to achieve promising performance in graph discovery for systems with up to 5 variables. Finally, we discuss benefits and drawbacks of the two algorithms.

2 Background and Related Work

2.1 Signature Kernels

Kernel methods are at the core of many key techniques in machine learning. A kernel defines a feature map that lifts observations into a (possibly infinite-dimensional) Hilbert space in which non-linear optimization problems on the original data often become linear and solutions can be expressed entirely in terms of kernel evaluations of the data. Selecting an effective kernel for a particular task and data modality is often challenging, particularly when the data is sequential. *Signature kernels* Király and Oberhauser (2019), Salvi et al. (2021a) are a class of *universal kernels* on sequential data which have received attention in recent years thanks to their efficiency in handling path-dependent problems Cirone et al. (2023), Cochrane et al. (2021), Issa et al. (2023), Lemercier et al. (2021), Salvi et al. (2021b,c).

The definition of the signature kernel requires an initial algebraic setup. Let $\langle \cdot, \cdot \rangle_1$ be the Euclidean inner product on \mathbb{R}^d . Denote by \otimes the standard tensor product of vector spaces.

For any $n \in \mathbb{N}$, the canonical Hilbert-Schmidt inner product $\langle \cdot, \cdot \rangle_n$ on $(\mathbb{R}^d)^{\otimes n}$ defined for any $a = (a_1, \dots, a_n)$ and $b = (b_1, \dots, b_n)$ in $(\mathbb{R}^d)^{\otimes n}$ as $\langle a, b \rangle_n = \prod_{i=1}^n \langle a_i, b_i \rangle_1$. Define the direct sum of vector spaces $T(\mathbb{R}^d) := \bigoplus_{n=1}^{\infty} (\mathbb{R}^d)^{\otimes n}$, where it is understood that the direct sum runs over finitely many non-zero levels. The inner product $\langle \cdot, \cdot \rangle_n$ on $(\mathbb{R}^d)^{\otimes n}$ can be extended by linearity to an inner product $\langle \cdot, \cdot \rangle$ on $T(\mathbb{R}^d)$ defined for any $a = (a_0, a_1, \dots)$ and $b = (b_0, b_1, \dots)$ in $T(\mathbb{R}^d)$ as $\langle a, b \rangle = \sum_{n=0}^{\infty} \langle a_n, b_n \rangle_n$. Other choices of linear extensions have been recently studied by [Cass et al. \(2023\)](#). We denote by $\mathcal{T}(\mathbb{R}^d)$ the Hilbert space obtained by completing $T(\mathbb{R}^d)$ with respect to $\langle \cdot, \cdot \rangle$.

The *signature transform*, a classical path-transform from stochastic analysis for any subinterval $[s, t] \subset [0, T]$ and any continuous path $X \in C_p([0, T], \mathbb{R}^d)$ of finite p -variation for $1 \leq p < 3$ is (canonically) defined by

$$S(X)_{s,t} := (1, S(X)_{s,t}^{(1)}, \dots, S(X)_{s,t}^{(n)}, \dots) \in \mathcal{T}(\mathbb{R}^d),$$

where $S(X)_{s,t}^{(n)} \in (\mathbb{R}^d)^{\otimes n}$ is the n -fold iterated integral

$$S(X)_{s,t}^{(n)} = \int_{s < u_1 < \dots < u_n < t} dX_{u_1} \otimes dX_{u_2} \otimes \dots \otimes dX_{u_n}.$$

The signature kernel

$$K_S : C_p([s, t], \mathbb{R}^d) \times C_p([s', t'], \mathbb{R}^d) \rightarrow \mathbb{R} \quad (2)$$

is the following symmetric function

$$K_S(X, Y) = \langle S(X)_{s,t}, S(Y)_{s',t'} \rangle.$$

A kernel-trick was derived by [Salvi et al. \(2021a\)](#), Theorem 2.5) who showed that the signature kernel satisfies the following path-dependent integral equation

$$f(t, t') = 1 + \int_s^t \int_{s'}^{t'} f(u, v) \langle dX_u, dY_v \rangle_1. \quad (3)$$

Several off-the-shelf python packages offer efficient PDE solvers for eq. (3) such as [sigkerax](#).

When restricted to compact sets in $C([0, T], \mathbb{R}^d)$, the signature kernel is characteristic ([Cass et al., 2023](#), Proposition 3.3), and this assumption can be relaxed further ([Chevyrev and Oberhauser, 2022](#)). Many results in kernel methods crucially depend on characteristic kernels, including tests for conditional independence ([Muandet et al., 2017](#)).

2.2 Conditional Independence Tests

Conditional independence (CI) is a fundamental notion in computational statistics and forms the foundation of graphical models. CI testing involves assessing whether two random variables, X and Y , are independent conditioned on a third random variables, Z , i.e., whether the null hypothesis $H_0 : X \perp\!\!\!\perp Y \mid Z$ can be rejected against the alternative $H_1 : X \not\perp\!\!\!\perp Y \mid Z$. When Z is discrete, conditional independence testing simplifies to a collection of unconditional tests for each value of Z ([Tsamardinou and Borboudakis, 2010](#)). When Z is continuous, most CI tests either rely on parametric assumptions about the underlying distributions ([Baba et al., 2004](#)) or rely primarily on kernel methods for nonparametric approaches ([Li and Fan, 2020](#), [Zhang et al., 2017](#)).

Kernel methods for CI testing typically leverage either kernel (ridge) regression or kernel mean embeddings and the Hilbert-Schmidt (conditional) independence criterion (HS(C)IC) to measure the reproducing kernel Hilbert space (RKHS) distance of the (conditional) mean embeddings of the joint distribution and the product of marginal distributions ([Gretton et al., 2007](#), [Muandet et al., 2017](#), [Park and Muandet, 2020](#)). Examples include KCIT ([Zhang et al.,](#)

2011) that draws on partial associations (Daudin, 1980) of regression functions connecting X , Y , Z , together with analytical or empirical (bootstrapped) expressions for the asymptotic distribution of the test statistic under the null. Strobl et al. (2019) approximate kernel computations in KCIT via random Fourier features for improved efficiency.

Other approaches rely on reducing CI to a two-sample test for the equivalent null $H_0 : P(X, Y, Z) = P(X | Z)P(Y | Z)P(Z)$. KCIPT (Doran et al., 2014) simulates samples from $P(X | Z)P(Y | Z)P(Z)$ by learning a permutation of the samples that approximately preserves Z values. Lee and Honavar (2017) propose a modified, unbiased estimate of the Maximum Mean Discrepancy (MMD) (Gretton et al., 2006) as the test statistic in KCIPT claiming improved calibration. Finally, other permutation-based approaches require large sample sizes (Sen et al., 2017) or rely on densities (Kim et al., 2022), which do not exist in our setting. Recently, Shah and Peters (2020) proposed a simple test based on double regression for increased robustness and later generalized this technique to a kernel-based regression techniques (Lundborg et al., 2022), which also applies to functional data via function-on-function ridge regressions. In our setting, these regressions are difficult to perform as they would have to map between arbitrary time segments of multivariate SDE solution paths. Laumann et al. (2023), perhaps the closest work to ours, develop a conditional independence test for functional data based on HSCIC (Park and Muandet, 2020) as the test statistic paired with a permutation test (Berrett et al., 2019). They further combine existing techniques such as the PC-algorithm (Glymour et al., 2019) with a regression-based method (Hoyer et al., 2008) for a causal discovery heuristic. Crucially, their method assumes knowledge of $P_{X|Z}$, a major challenge in our SDE setting. We focus on constraint-based methods leveraging the ability of the signature kernel to capture filtrations on arbitrary intervals. Since Laumann et al. (2023) propose the only other method we are aware of that can be applied in our setting, we benchmark our CI test against them.

On a practical level, large conditioning sets inevitably imply curse-of-dimensionality type issues as the ‘number possible values to condition on’ grows exponentially. Moreover, existing approaches often assume observations in real Euclidean vector spaces and do not directly generalize to path-valued random variables where no densities exist. On a theoretical level, CI testing faces a fundamental impossibility in that there cannot be a universally powerful test for all distributions while also controlling the type I error (Lundborg et al., 2022, Shah and Peters, 2020). This ‘no free lunch’ statement highlights the importance of carefully selecting an appropriate test for the setting under consideration. Currently, there exists no practical CI test tailored to our case—a gap we fill.

2.3 Causal Discovery on Time Series

Discrete-time models generally rely on explicit functional relations between variables across a fixed homogeneous time grid, i.e., $X_t = f(X_{t-\tau}, \dots, X_{t-1})$. This can be interpreted as a static structural causal model (SCM) over the ‘unrolled graph’, where variables at different time steps are considered as distinct nodes (Peters et al., 2017). The direction of time implies that edges across time steps can only point into the future (a maximum ‘lookback window’, $\tau \in \mathbb{N}$, is common). This has been exploited in Granger-type approaches (Eichler, 2007, Eichler and Didelez, 2010). Related techniques for causal discovery in the discrete-time model include constraint-based methods (Runge et al., 2023, 2019, 2020) with extensions to scenarios lacking causal sufficiency (Entner and Hoyer, 2010, Gerhardus and Runge, 2020, Malinsky and Spirtes, 2018), and score-based methods (Pamfil et al., 2020). Based on Granger causality (Granger, 1969), different works detect lagged causal influences in linear (Diks and Panchenko, 2006, Granger, 1980) or non-linear (Marinazzo et al., 2008, Runge, 2020, Shojaie and Fox, 2022) functional relationships. Due to the fundamental challenges encountered in discrete-time systems (Runge, 2018), causal modeling in continuous-time dynamical systems has received increasing attention.

A growing body of work considers differential equations at equilibrium to obtain ‘solvable’ structural causal models that may include cycles (Bongers et al., 2018, Bongers and Mooij, 2018, Mooij et al., 2013). Due to their assumptions about the data generating mechanism, this work does not apply to our setting. Other works instead aim at learning the full dynamical law by leveraging invariance under the assumption of mass-action-kinetics (Peters et al., 2022) or relying on non-convex optimization of heavily overparameterized neural network models for reconstruction performance (Aliee et al., 2022, 2021, Bellot et al., 2022). In continuous-time stochastic processes, so-called (*conditional*) *local independence* defines an asymmetric independence relation (Mogensen et al., 2018, Schweder, 1970). Tests of local independence may be used to learn a (partial) causal graph in, e.g., point process models and diffusions (Didelez, 2008, Meek, 2014, Mogensen and Hansen, 2020, Mogensen et al., 2018).

3 Method

3.1 Causal Discovery in the Acyclic SDE Model

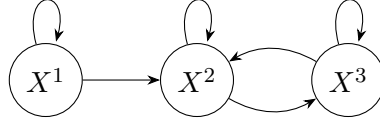
Assumption 3.1. We assume the existence of a conditional independence oracle for statements of the form

$$X_{\mathcal{I}}^I \perp\!\!\!\perp X_{\mathcal{J}}^J \mid X_{\mathcal{K}}^K \quad (4)$$

for disjoint $I, J, K \subset \{1, \dots, d\}$ where only K may be empty, closed intervals $\mathcal{I}, \mathcal{J}, \mathcal{K} \subset [0, T]$, and where $X_{[a,b]}^H$ denotes the $C([a, b], \mathbb{R}^{|H|})$ -valued random variable $\omega \mapsto ([a, b] \ni t \mapsto X_t^h(\omega)^{h \in H})$. We assume access to finitely but arbitrarily many queries to the oracle.

Asymptotically, such an oracle can realistically be replaced in practice by a consistent finite-sample CI test for path-valued random variables (see Section 3.2). The following example demonstrates that constraint-based causal discovery of the full dependency graph is impossible using just Assumption 3.1 when allowing for cycles.

Example 3.2. The oracle in Assumption 3.1 is not powerful enough to rule out a directed edge $X^1 \rightarrow X^3$ for an SDE model with the following dependency graph:



We go through this example and describe a different type of oracle that would be required for causal discovery in cyclic SDE models in Appendix A.2. Example 3.2 provides additional motivation for considering acyclic SDE models, still allowing for loops. Loops are crucial in the dynamic setting, as they represent dependencies of a variable on itself, infinitesimally into the past.

We will use the oracle in three distinct ways ($i, j \in [d]$, $K \subset [d]$, $\{i, j\} \cap K = \emptyset$):

- X^i is *symmetrically conditionally independent* of X^j given X^K on $[0, T]$, $X^i \perp\!\!\!\perp_{\text{sym}} X^j \mid X^K$ if

$$X_{[0,T]}^i \perp\!\!\!\perp X_{[0,T]}^j \mid X_{[0,T]}^K$$

- X^i is *future-extended h -locally conditionally independent* of X^j given X^K at s , $X^i \perp\!\!\!\perp_{s,h}^+ X^j \mid X^K$ if²

$$X_{[0,s]}^i \perp\!\!\!\perp X_{[s,s+h]}^j \mid X_{[0,s]}^j, X_{[0,s+h]}^K$$

²The ‘+’ superscript is meant to emphasise the fact that we are also conditioning on the future of X^K , which is not usually done (cf. the definition of global non-causality in Florens and Fougeré (1996)), and is motivated by our causal discovery procedure.

- X^i is conditionally h -locally self-independent given X^K at s , $X^i \perp\!\!\!\perp_{s,h}^\circ | X^K$ if

$$X_{[0,s]}^i \perp\!\!\!\perp X_{[s,s+h]}^i | X_{[0,s+h]}^K$$

We will only need to work on two intervals, $[0, s]$ and $[s, s + h]$, with $h > 0$. Define the *lifted* dependency graph $\tilde{\mathcal{G}} = (\tilde{V}, \tilde{E})$ by setting $\tilde{V} := V_0 \sqcup V_1$, where \sqcup denotes disjoint union and V_0, V_1 are two copies of V , whose elements we subscript with 0 and 1; include an edge $(i_0 \rightarrow i_1) \in \tilde{E}$ iff there is a loop $(i \rightarrow i) \in E$, and for each edge $(i \rightarrow j) \in E$ with $i \neq j$, include edges $(i_0 \rightarrow j_0), (i_1 \rightarrow j_1), (i_0 \rightarrow j_1) \in \tilde{E}$. Conversely, we say that the graph with edges E is obtained by *collapsing* the graph with edges \tilde{E} .

Proposition 3.3 (Markov property). *Assume \mathcal{G} is directed and acyclic except for loops. Then $\tilde{\mathcal{G}}$ is acyclic, and the assignment of $X_{[0,s]}^i$ to the node i_0 and $X_{[s,s+h]}^i$ to i_1 , for each $i \in V$ defines a fully observed SCM (Peters et al., 2017). In particular, its observational distribution satisfies the global Markov property w.r.t. to $\tilde{\mathcal{G}}$.³*

Our proof is in Appendix A.3. Under Assumption 3.1 and assuming faithfulness for the SCM of Proposition 3.3, we now develop modified versions of the PC algorithm. More details on faithfulness and minimality can be found in Appendix A.4.

Algorithm 1 Causal discovery for acyclic SDE models.

```

1:  $\tilde{V} \leftarrow \{k_0, k_1 \mid k \in V\}$ 
    $\tilde{E} \leftarrow \{i_0 \rightarrow j_0, i_1 \rightarrow j_1 \mid i, j \in V, i \neq j\}$ 
       $\cup \{i_0 \rightarrow j_1 \mid i, j \in V\}$ 
2: for  $c = 0, \dots, d - 2$  do ▷ edge recovery modulo loops
3:   for  $i, j \in V, i \neq j$  do
4:     for  $K \subseteq V \setminus \{i, j\}, |K| = c,$ 
5:       s.t.  $(k_0 \rightarrow j_1) \in \tilde{E}$  for  $k \in K$  do
6:         if  $X^i \perp\!\!\!\perp_{s,h}^+ X^j | X^K$  then
7:            $\tilde{E} \leftarrow \tilde{E} \setminus \{i_0 \rightarrow j_0, i_1 \rightarrow j_1, i_0 \rightarrow j_1\}$ 
8:    $\mathcal{G} = (V, E) \leftarrow \text{collapse}(\tilde{V}, \tilde{E})$ 
9:   for  $k \in V$  do ▷ removing loops
10:    if  $X^k \perp\!\!\!\perp_{s,h}^\circ | X^{\text{pa}_k^{\mathcal{G}} \setminus \{k\}}$  then
11:       $E \leftarrow E \setminus \{k \rightarrow k\}$ 
12: return  $\mathcal{G}$ 

```

Discovering the full DAG \mathcal{G} . To discover the full graph including loops we propose Algorithm 1 that makes use of the time-ordering via our h -local independence models (consider $s, h > 0$ arbitrary but fixed). Algorithm 1 is kept conceptually simple and not an optimized version. As suggested by Spirtes et al. (2000), we could for instance restrict the conditioning set (K) to nodes that lie on undirected paths between i and j or introduce an additional for-loop that slowly grows the cardinality of the conditioning set in the second stage (line 8 of Algorithm 1 as well).

Theorem 3.4 (Causal discovery for acyclic SDEs). *Algorithm 1 is sound and complete for the SDE model eq. (1), assuming acyclicity except for loops and faithfulness: its output coincides with the dependency graph \mathcal{G} of the SDE.*

The proof of the theorem can be found in Appendix A.6.

Remark 3.5. If we knew in advance that there is no path-dependency, the test $X^i \perp\!\!\!\perp_{s,h}^+ X^j$ (with no additional conditioning set) is equivalent to the test on values of the process $X_s^i \perp\!\!\!\perp X_{s+h}^j | X_s^j$: this is because X_u^j , for $u \in [s, t]$ only depends on $X_{[s,t]}^j$ via X_s^j . However, this kind of statement no longer works in the conditional case (by arguments similar to Example 3.2), and testing on whole paths is strictly necessary when allowing for path-dependency.

³We use the term *Markov* for the Markov property in causality, not as in ‘Markov process’.

Remark 3.6. CI testing of SDEs is conceptually similar to static CI on discretely sampled data, when the sampling rate is lower than the actual frequency at which causal effects propagate. This is because, in continuous time and for any $h > 0$, there are going to be causal effects that occur at time scales less than h . Whenever we just discretely sample time series with no instantaneous effects, [Peters et al. \(2017, Thm. 10.3\)](#) provides full causal discovery, even in the presence of cycles in the summary graph, by performing d^2 tests $X_s^i \perp\!\!\!\perp X_{s+\Delta_s}^j \mid X_{[0,s]}^{[d]\setminus\{i,j\}}$. Potentially absent loops could then be removed as in [Algorithm 1](#). Ignoring that this might suffer from the conditioning set being too large, our signature method can be of help in this setting too, if there is path-dependence: the conditioning variable can be taken to be $S(X^{[d]\setminus\{i,j\}})_{0,s}$.

Discovering and post-processing the CPDAG. Besides causal discovery of the full DAG \mathcal{G} using the asymmetric future-extended h -local independence criterion, we also propose a constraint-based causal discovery algorithm based on the symmetric independence condition that recovers the completed partially directed acyclic graph (CPDAG) of \mathcal{G} with self-loops removed, which represents the Markov equivalence class of \mathcal{G} ([Peters et al., 2017](#)). We present the algorithm together with a soundness and completeness proof in [Appendix A.7](#). While [Algorithm 1](#) is ‘stronger’ in that it orients all edges, it (a) typically requires more CI tests, (b) has larger conditioning sets in the $\perp\!\!\!\perp_{s,h}^+$ -CI tests, (c) requires the choice of a extra parameters s, h for $\perp\!\!\!\perp_{s,h}^+$, (d) runs CI tests on shorter time segments, potentially ‘losing information’ compared to the symmetric test $\perp\!\!\!\perp_{\text{sym}}$. All these factors empirically negatively affect the reliability of the CI test, which may indicate that causal discovery of the CPDAG using $\perp\!\!\!\perp_{\text{sym}}$ may be more reliable, despite yielding a weaker result at first.

Given these potential benefits, we propose to further augment the CPDAG discovery by a post-processing step in which we aim at orienting all remaining unoriented edges (i, j) within the Markov equivalence class represented by the CPDAG leveraging the following corollary.

Corollary 3.7 (post-processing). *Let $X = (X^1, \dots, X^d)$ be a stochastic process satisfying the SDE in [eq. \(1\)](#) such that the induced graph $\mathcal{G} = (V, \mathcal{E})$ is a DAG. Let $\tilde{\mathcal{G}} = (V, \tilde{\mathcal{E}})$ be the CPDAG representing the Markov equivalence class of \mathcal{G} . Then for all $(i, j) \in \mathcal{E} \subset \tilde{\mathcal{E}}$ with $(j, i) \in \tilde{\mathcal{E}}$ and $i \neq j$ it holds that $X_{[0,T]}^j \not\perp\!\!\!\perp X_0^i$ but $X_{[0,T]}^i \perp\!\!\!\perp X_0^j$.*

This allows us to determine the orientation of remaining edges in a post-processing step that crucially only requires unconditional independence tests only for the edges that are not yet oriented in the CPDAG. Hence, we obtain an alternative algorithm to discover the full graph that is sound and complete under the oracle assumption and faithfulness by (a) constructing the CPDAG with the PC-algorithm using $\perp\!\!\!\perp_{\text{sym}}$, and (b) a post-processing step where we test the unconditional independencies in [Corollary 3.7](#) for all unoriented edges. We compare both versions in our experiments.

3.2 Signature Kernel Conditional Independence Test

Our theoretical results in [Section 3.1](#) make use of the assumption of a CI oracle. To make our proposed algorithms practically applicable, we propose a flexible and powerful CI test on path-valued random variables (on different time intervals), i.e., the conditions in [Assumption 3.1](#). The general idea of using the signature kernel for kernel-based hypothesis tests for stochastic processes has recently also been proposed by [Chevyrev and Oberhauser \(2022\)](#), [Salvi et al. \(2021c\)](#), but has been limited to standard two-sample tests or conditional independence tests that do not take into account time ordering. The idea of using terms of the signature to detect causality (not specifically with hypothesis testing) was also proposed in [Giusti and Lee \(2020\)](#) and developed further in [Glad and Woolf \(2021\)](#). Assume we have observed n samples of (potentially multi-variate) path segments $X_{\mathcal{I}}^{(i)}$, $Y_{\mathcal{J}}^{(i)}$, and $Z_{\mathcal{K}}^{(i)}$ of components X, Y, Z of a stochastic process on arbitrary intervals $\mathcal{I}, \mathcal{J}, \mathcal{K} \subset [0, T]$ for $i \in [n]$. Using the signature kernel K_S we compute the Gram matrices $k_{XX}, k_{YY}, k_{ZZ} \in \mathbb{R}^{n \times n}$ for these n samples, based

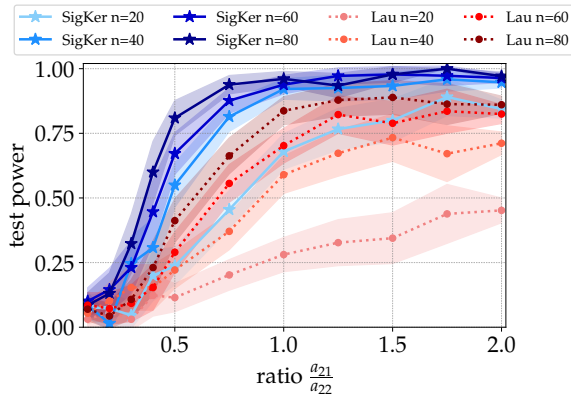


Figure 2: Test power when testing $H_0 : X_{[0,t]}^1 \not\perp\!\!\!\perp X_{[0,t]}^2$ for different ratios $\frac{a_{21}}{a_{22}}$ in the bivariate setting $X^1 \rightarrow X^2$, where our CI test (SigKer) consistently outperforms the baseline from Laumann et al. (2023) (Lau). Lines show means over 1000 SDEs (see main text) and shaded regions show standard errors.

Table 1: SHD ($\times 10^2$) results of our method (SigKer) and the baselines CCM, PCMCI and Granger causality in four different bivariate settings: linear SDEs, path-dependent SDEs, non-linear SDEs and SDEs with diffusion dependency.

($\times 10^2$)	linear		path-dependent		non-linear		diffusion dependency	
	$n = 200$	$n = 400$	$n = 200$	$n = 400$	$n = 200$	$n = 400$	$n = 200$	$n = 400$
CCM	100.1 \pm 5.0	78.9 \pm 4.9	107.7 \pm 4.9	138.5 \pm 4.6	19.8 \pm 3.0	15.8 \pm 2.7	79.2 \pm 4.9	76.7 \pm 4.8
Granger	103.0 \pm 2.5	116.7 \pm 2.2	92.3 \pm 1.9	100.0 \pm 2.4	54.4 \pm 3.6	57.4 \pm 3.8	95.0 \pm 2.7	89.1 \pm 2.4
PCMCI	125.9 \pm 4.8	55.5 \pm 4.4	88.1 \pm 4.4	114.7 \pm 4.4	71.3 \pm 2.3	85.1 \pm 1.7	74.3 \pm 2.2	90.0 \pm 1.5
SigKer	82.4 \pm 1.9	28.6 \pm 2.8	52.7 \pm 2.4	24.3 \pm 2.1	11.1 \pm 1.6	0.0 \pm 0.0	74.3 \pm 2.1	62.5 \pm 2.3

on which we can directly run kernel-based permutation CI tests such as KCIPT (Doran et al., 2014) or SDCIT (Lee and Honavar, 2017) to test $X_{\mathcal{I}} \perp\!\!\!\perp Y_{\mathcal{J}} \mid Z_{\mathcal{K}}$. While the existing consistency proof for KCIPT (also applying to SDCIT) makes use of the existence of a density, we extend this proof to path-valued random variables.

Theorem 3.8 (informal). *KCIPT with the signature kernel on path-space is consistent for the tests in Assumption 3.1.*

We provide the precise conditions and a proof in Appendix A.8. While such consistency proofs provide theoretical grounding, as described in Section 2, CI tests must be carefully selected and validated in a given domain empirically. Therefore, the extensive evaluation of our CI test in the next section is perhaps more important in practice.

4 Experiments

First, we compare how different kernel-based CI tests perform in conjunction with the signature kernel in Appendix C. Based on results in Figure 5 and the consistency statement in Theorem 3.8, we use KCIPT in all subsequent experiments.

Baselines. We compare against established causal discovery methods in time series, specifically CCM (Sugihara et al., 2012), PCMCI (Runge et al., 2019), Granger causality (Granger, 1969), and the recent approach by Laumann et al. (2023). CCM and Granger causality are restricted to bivariate settings and Laumann et al. (2023) conditional independence test requires additional knowledge about the underlying distribution and is therefore not suited for a comparison outside the unconditional case. Details about the baseline implementations are in Appendix C.

Table 2: Test performance on the key building blocks for causal discovery. Here, $\perp\!\!\!\perp$ refers to $\perp\!\!\!\perp_{\text{sym}}$ except for $X_p^1 \perp\!\!\!\perp X_f^1$ which means $X_{[0,t/2]}^1 \perp\!\!\!\perp X_{[t/2,t]}^1$. We use KCIPT for CI tests and bootstrapped HSIC unconditional independence. We simulate 40 samples of 512 trajectories for 10 different SDEs (400 tests per column) with 25% of the 128 original observations dropped uniformly at random. The **error** represent type I or type II error when the null hypothesis H_0 should be rejected (\times) or accepted (\checkmark), respectively.

graph										
H_0	$X^1 \perp\!\!\!\perp X^2 X^3$	$X^1 \perp\!\!\!\perp X^3 X^2$	$X^1 \perp\!\!\!\perp X^2 X^3$	$X^1 \perp\!\!\!\perp X^3 X^2$	$X^1 \perp\!\!\!\perp X^3 X^2$	$X^1 \perp\!\!\!\perp X^2$	$X^1 \perp\!\!\!\perp X^3$	$X^1 \perp\!\!\!\perp X^2$	$X^1 \perp\!\!\!\perp X^3$	$X^1 \perp\!\!\!\perp X^2$
should reject	\checkmark	\times	\checkmark	\checkmark	\times	\checkmark	\times	\checkmark	\times	\checkmark
error	0.0025	0.1775	0.0000	0.0025	0.1250	0.0000	0.0450	0.0000	0.0450	0.0000

Metrics, model choices, hyperparameters. In all experiments, we use KCIPT for conditional and the permutation-based version of HSIC for unconditional tests. We use `sigkerax` for the signature kernel with an RBF lifting kernel that operates pointwise on sequences. The length scale is selected via a median heuristic on pairwise Euclidean distances between all observed time points across all samples, which we motivate in Appendix B.1. In all bivariate settings, we fix the causal structure as $X^1 \rightarrow X^2$ and generate multiple SDEs from which we sample different numbers of trajectories. For causal discovery in $d \in \{3, 4, 5\}$, the DAG adjacency structures are sampled from a Erdős–Rényi model with edge probability 0.7. Following the causal discovery literature, we compute the Structural Hamming Distance (SHD) as our main performance metric, where correctly predicting the absence of an edge or a correctly oriented edge counts 0, predicting an edge where there should be none or vice versa adds 1, and predicting an edge in the wrong direction counts 2 (see Appendix B.7). Except for non-linear experiments, the assumed SDE model is $(A, B \in \mathbb{R}^{d \times d}$ and $c, d \in \mathbb{R}^d)$

$$dX_t = (AX_t + c)dt + \text{Diag}(BX_t + d)dW_t. \quad (5)$$

4.1 Power Analysis of the Bivariate Independence Test

In the first series of experiments, we measure the test power using the unconditional test in the case $X^1 \rightarrow X^2$ for SDEs of the form eq. (5), with constant diffusion $B \equiv 0$, $d_i = 0.4$

Figure 2 shows that test power swiftly approaches 1 for as few as 40-60 samples as the ratio between causal- and self-interaction strength $\frac{a_{21}}{a_{22}}$ at X^2 increases, so as soon as the causal interaction of X^1 feeding into X^2 reaches a substantial level compared to X^2 self-driven dynamics. Our method consistently outperforms Laumann et al. (2023) across sample sizes. In addition, since the signature kernel naturally handles irregularly observed paths, Figure 6 shows that our test also consistently outperforms the baselines even at high levels of data missingness (for details see Appendix B.4).

4.2 Leveraging the Direction of Time

Next, we explore a bivariate scenario with $X^1 \rightarrow X^2$, where we leverage the direction of time to orient the edge using the future-extended h-local conditional independence with $K = \emptyset$ for different interaction types.

Linear case. In the case of linear drift-interaction, SDEs are drawn from eq. (5) with $a_{21} \sim \mathcal{U}([0.8, 1])$, $a_{11}, a_{22} \sim \mathcal{U}([0, 0.5])$, $a_{12} = 0$, $B \equiv 0$, $d_i \sim \mathcal{U}([0.3, 0.4])$. Table 1 (setting *linear*) shows that our criterion not only accurately captures the presence of the edge but also captures the direction of dependence for sufficient amounts of samples, outperforming both CCM, Granger causality and PCMCI.

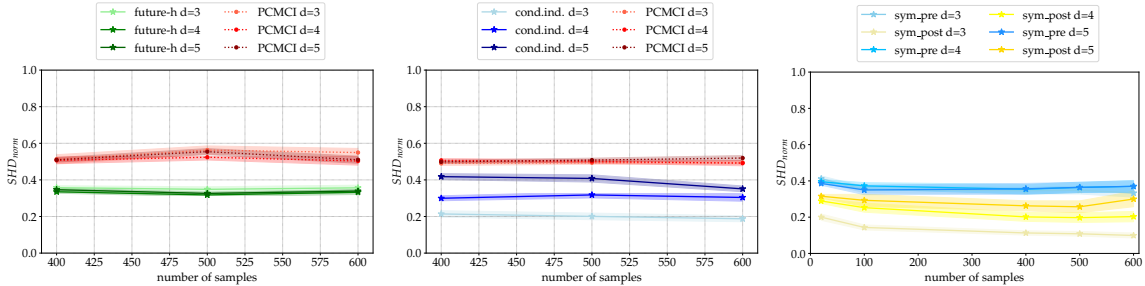


Figure 3: SHD_{norm} on predicted graphs over sample sizes for different numbers of nodes d . **Left:** Full graph discovery using Algorithm 1 compared to PCMCi (evaluated against the full ground truth graph). **Middle:** CPDAG discovery with the PC-algorithm and \perp_{sym} compared to PCMCi (evaluated against the CPDAG of the ground truth graph). **Right:** Full graph discovery by post-processing the CPDAG via Corollary 3.7 (evaluated against the full ground truth graph without loops). We outperform PCMCi both in inferring the full graph (with both methods) and in inferring the CPDAG. Post-processing the CPDAG performs best across settings, arguably due to the comparably ‘simple’ and fewer (conditional) independence tests required. Lines are means of SHD and shaded areas standard deviations over 100 settings.

Path-dependent case. Sampling from the 3-dimensional SDE in eq. (5), with $B \equiv 0$, $c \equiv 0$, all entries of A being zero except $a_{23}, a_{31} \sim \mathcal{U}([1, 1.1])$ and $d = (d_1, d_2, 0)^\top$, $d_i \sim \mathcal{U}([0.3, 0.4])$ effectively generates a bivariate scenario $X^1 \rightarrow X^2$ with a path-dependency in X^2 of the form $dX_t^2 = \mu^2(X_{[0,t]}^1)dt + d_2dW_t^1$. Denoted by setting *path-dependent*, Table 1 again shows that the criterion captures the direction of dependence better than CCM, PCMCi and Granger.

Non-linear case. Our proposed criterion is also able to almost perfectly predict the graph for non-linear SDEs as

$$d \begin{pmatrix} X_t^1 \\ X_t^2 \end{pmatrix} = \begin{pmatrix} -r\omega \sin(\omega t) \\ r\omega \tanh(X_t^2) \end{pmatrix} dt + \text{Diag}(d^\top)dW_t$$

where $\nu \sim \mathcal{U}([3, 4])$, $\omega = 2\pi\nu$, $r \sim \mathcal{U}([2, 2.5])$ and $d_i \sim \mathcal{U}([0.3, 0.4])$, outperforming the baselines (see Table 1).

Diffusion case. In the final bivariate experiment, we test the prediction-capability of our independence criterion in setting (5) where all entries of A, B are zero except for $a_{11}, a_{22} \sim \mathcal{U}([0.5, 1])$ and $b_{21} \sim \mathcal{U}([2.5, 3])$, and $d \equiv 0$. As the only method capable of handling this type of dependence, we again outperform the baselines (see Table 1).

4.3 Building Blocks for Causal Discovery

The performance of the conditional and unconditional independence tests was evaluated using widely recognized causal structures that are at the foundation of causal discovery. Specifically, we examined scenarios involving two variables, both connected and unconnected, and three-variable configurations comprising chain, fork, and collider structures. More details on the experiments are found in Appendix B.5. The analysis of type I and type II errors, as shown in Table 2, indicates robust performance for both conditional KCIPT and unconditional HSIC tests. These results refer to the symmetric conditional independence \perp_{sym} , while future-extended h-local conditional independence are presented in Table 6. In Appendix B.5, further results in the diffusion dependency setting (Table 5).

4.4 Causal Discovery in Higher Dimensions

After having dealt with the bivariate case and the building blocks of causal discovery, we now test the performance of our CI test in conjunction with our causal discovery algorithms.

Table 3: Comparison of pairs trading performance metrics demonstrating superiority of our method over ADF, Granger, and their combined approach (ADF & Granger) in most metrics. The symbol \uparrow indicates ‘higher is better’, while \downarrow signifies ‘lower is better’.

	return \uparrow	APR \uparrow	Sharpe \uparrow	maxDD \downarrow	maxDDD \downarrow
ADF	0.004	0.004	0.090	0.087	230
Granger	-0.010	-0.011	-0.230	0.056	219
ADF & Granger	0.008	0.008	0.242	0.022	153
SigKer (ours)	0.076	0.077	1.500	0.027	21

We sample 100 DAG adjacency structures for dimensions $d \in \{3, 4, 5\}$ and draw samples from d -dimensional SDEs as in (5) satisfying this given adjacency structure and $a_{ij} \sim \mathcal{U}([-2, -1] \cup [1, 2])$, $j \neq i$, $a_{ii} \sim \mathcal{U}([-0.5, 0.5])$.

First, we run our full graph discovery Algorithm 1 and show in Figure 3(left) that it consistently outperforms PCMCI on full graph discovery (including loops). We then test the symmetric CI criterion $\perp\!\!\!\perp_{\text{sym}}$ with the regular PC-algorithm (sound and complete as shown in Appendix A.7). We evaluate the found CPDAG against the ground truth DAG via the normalized SHD without testing for self-loops. Figure 3(middle) shows that across all evaluated dimensions and sample sizes, our method consistently outperforms PCMCI. Note that in this comparison, we only consider whether the CPDAG has been predicted correctly, i.e., the SHD_{norm} is less stringent in this case compared to a full DAG comparison. In Figure 3(right), we then show how the inferred CPDAGs match the ground truth DAG (now SHD_{norm} compares to the actual ground truth DAG) and how much we gain from the post-processing step that aims at orienting remaining unoriented edges. The ultimate performance of the post-processed CPDAG is the strongest in our empirical findings.

4.5 Real-World Pairs Trading Example

Finally, we apply our method on real-world data for evaluating pair trading strategies on ten stocks from the VBR Small-Cap ETF over a three-year period from January 1, 2010, to December 31, 2012. While financial data typically lacks a ground truth for validation, we assess the effectiveness of our method by quantifying the product-and-loss (P&L) profile of the pair trading strategy generated via our model. We select pairs based on the pairwise p-values of different hypothesis tests: 1) cointegration, tested via the classical Augmented Dickey-Fuller (ADF) test, 2) classical Granger causality test and 3) our method. As shown in Table 3, the P&L of our trading strategy outperforms the P&L of the two benchmarks in terms of most classical trading metrics: total return, APR, Sharpe ratio, maxDDD. More details on the implementation can be found in Appendix B.6.

5 Conclusions and Future Work

In this work, we introduced a kernel-based test for conditional independence on path-space, utilizing signature kernels, and applied it to constraint-based causal discovery in stochastic dynamical systems. We developed an algorithm for comprehensive causal discovery in acyclic systems. This algorithm operates under the assumptions of faithfulness and the availability of a conditional independence oracle.

To deploy this algorithm in practice, we developed a consistent conditional independence test based on the signature kernel and extensively evaluated its performance empirically. Our results indicate that our method outperforms existing baselines for causal discovery on time series, highlighting its potential in complex dynamic systems. Additionally, we successfully

applied our method to a real-world pairs trading example, where it also demonstrated strong performance.

An interesting direction for future work involves extending our approach to cyclic settings and accommodating dynamics with temporally changing causal structure or with partial observations. Future research could expand on these applications in real-world scenarios, to evaluate the method's practical impact in concrete domains. Moreover, the field of causality represents just one of the many potential applications of conditional independence tests for path-valued random variables. Exploring other applications in different domains could also catalyze new insights and developments.

Acknowledgments

Cecilia Casolo is supported by the DAAD programme Konrad Zuse Schools of Excellence in Artificial Intelligence, sponsored by the Federal Ministry of Education and Research. Emilio Ferrucci is supported by UKRI EPSRC Programme Grant EP/S026347/1. Søren Wengel Mogensen is supported by Independent Research Fund Denmark (DFE-International Postdoctoral Grant 0164-00023B) and a member of the ELLIIT Strategic Research Area at Lund University.

References

- Aliee, H., Richter, T., Solonin, M., Ibarra, I., Theis, F., and Kilbertus, N. (2022). Sparsity in continuous-depth neural networks. *Advances in Neural Information Processing Systems*, 35:901–914. [6](#)
- Aliee, H., Theis, F. J., and Kilbertus, N. (2021). Beyond predictions in neural odes: Identification and interventions. *arXiv preprint arXiv:2106.12430*. [6](#)
- Annadani, Y., Pawlowski, N., Jennings, J., Bauer, S., Zhang, C., and Gong, W. (2023). Bayesdag: Gradient-based posterior sampling for causal discovery. *arXiv preprint arXiv:2307.13917*. [1](#)
- Assaad, C. K., Devijver, E., and Gaussier, E. (2022). Discovery of extended summary graphs in time series. In *Uncertainty in Artificial Intelligence*, pages 96–106. PMLR. [2](#)
- Baba, K., Shibata, R., and Sibuya, M. (2004). Partial correlation and conditional correlation as measures of conditional independence. *Australian & New Zealand Journal of Statistics*, 46(4):657–664. [4](#)
- Bellot, A., Branson, K., and van der Schaar, M. (2022). Neural graphical modelling in continuous-time: consistency guarantees and algorithms. In *International Conference on Learning Representations*. [6](#)
- Berrett, T., Wang, Y., Barber, R., and Samworth, R. (2019). The conditional permutation test for independence while controlling for confounders. *Journal of the Royal Statistical Society: Series B (Statistical Methodology)*, 82. [5](#)
- Bongers, S., Blom, T., and Mooij, J. M. (2018). Causal modeling of dynamical systems. *arXiv preprint arXiv:1803.08784*. [6](#)
- Bongers, S., Forré, P., Peters, J., and Mooij, J. M. (2021). Foundations of structural causal models with cycles and latent variables. *The Annals of Statistics*, 49(5):2885 – 2915. [21](#), [32](#)
- Bongers, S. and Mooij, J. M. (2018). From random differential equations to structural causal models: The stochastic case. *arXiv preprint arXiv:1803.08784*. [6](#)
- Brouillard, P., Lachapelle, S., Lacoste, A., Lacoste-Julien, S., and Drouin, A. (2020). Differentiable causal discovery from interventional data. *Advances in Neural Information Processing Systems*, 33:21865–21877. [1](#)
- Cass, T., Lyons, T., and Xu, X. (2023). Weighted signature kernels. *Annals of Applied Probability*. [4](#), [26](#)
- Charpentier, B., Kibler, S., and Günnemann, S. (2022). Differentiable DAG sampling. In *International Conference on Learning Representations*. [1](#)
- Chen, H., Du, K., Yang, X., and Li, C. (2022). A review and roadmap of deep learning causal discovery in different variable paradigms. *arXiv preprint arXiv:2209.06367*. [1](#)

- Chevyrev, I. and Oberhauser, H. (2022). Signature moments to characterize laws of stochastic processes. *J. Mach. Learn. Res.*, 23(1). 4, 8
- Christgau, A. M., Petersen, L., and Hansen, N. R. (2023). Nonparametric conditional local independence testing. *The Annals of Statistics*, 51(5):2116 – 2144. 22
- Cirone, N. M., Lemerrier, M., and Salvi, C. (2023). Neural signature kernels as infinite-width-depth-limits of controlled resnets. In *Proceedings of the 40th International Conference on Machine Learning*, ICML’23. JMLR.org. 3
- Cochrane, T., Foster, P., Chhabra, V., Lemerrier, M., Lyons, T., and Salvi, C. (2021). Sk-tree: a systematic malware detection algorithm on streaming trees via the signature kernel. In *2021 IEEE international conference on cyber security and resilience (CSR)*, pages 35–40. IEEE. 3
- Daudin, J. (1980). Partial association measures and an application to qualitative regression. *Biometrika*, 67(3):581–590. 5
- Didelez, V. (2008). Graphical models for marked point processes based on local independence. *Journal of the Royal Statistical Society: Series B (Statistical Methodology)*, 70(1):245–264. 6
- Diks, C. and Panchenko, V. (2006). A new statistic and practical guidelines for nonparametric granger causality testing. *Journal of Economic Dynamics and Control*, 30(9-10):1647–1669. 5
- Doran, G., Muandet, K., Zhang, K., and Schölkopf, B. (2014). A permutation-based kernel conditional independence test. In *UAI*, pages 132–141. 5, 9, 26, 27, 29
- Eichler, M. (2007). Granger causality and path diagrams for multivariate time series. *Journal of Econometrics*, 137(2):334–353. 5
- Eichler, M. and Didelez, V. (2010). On granger causality and the effect of interventions in time series. *Lifetime data analysis*, 16:3–32. 5
- Entner, D. and Hoyer, P. O. (2010). On causal discovery from time series data using fci. *Probabilistic graphical models*, pages 121–128. 5
- Evans, L. C. (2006). An introduction to stochastic differential equations version 1.2. *Lecture Notes, UC Berkeley*. 2
- Florens, J.-P. and Fougere, D. (1996). Noncausality in continuous time. *Econometrica: Journal of the Econometric Society*, pages 1195–1212. 6, 22
- Gégout-Petit, A. and Commenges, D. (2010). A general definition of influence between stochastic processes. *Lifetime data analysis*, 16(1):33–44. 22
- Gerhardus, A. and Runge, J. (2020). High-recall causal discovery for autocorrelated time series with latent confounders. *Advances in Neural Information Processing Systems*, 33:12615–12625. 5
- Giusti, C. and Lee, D. (2020). Iterated integrals and population time series analysis. In Baas, N. A., Carlsson, G. E., Quick, G., Szymik, M., and Thaulé, M., editors, *Topological Data Analysis*, pages 219–246, Cham. Springer International Publishing. 8
- Glad, W. and Woolf, T. (2021). Path signature area-based causal discovery in coupled time series. In Ma, S. and Kummerfeld, E., editors, *Proceedings of The 2021 Causal Analysis Workshop Series*, volume 160 of *Proceedings of Machine Learning Research*, pages 21–38. PMLR. 8

- Glymour, C., Zhang, K., and Spirtes, P. (2019). Review of causal discovery methods based on graphical models. *Frontiers in genetics*, 10:524. [1](#), [5](#)
- Granger, C. W. (1969). Investigating causal relations by econometric models and cross-spectral methods. *Econometrica: journal of the Econometric Society*, pages 424–438. [5](#), [9](#)
- Granger, C. W. (1980). Testing for causality: A personal viewpoint. *Journal of Economic Dynamics and control*, 2:329–352. [5](#)
- Gretton, A., Borgwardt, K., Rasch, M., Schölkopf, B., and Smola, A. (2006). A kernel method for the two-sample-problem. *Advances in neural information processing systems*, 19. [5](#)
- Gretton, A., Fukumizu, K., Teo, C., Song, L., Schölkopf, B., and Smola, A. (2007). A kernel statistical test of independence. *Advances in neural information processing systems*, 20. [4](#), [29](#)
- Hägele, A., Rothfuss, J., Lorch, L., Somnath, V. R., Schölkopf, B., and Krause, A. (2023). Bacadi: Bayesian causal discovery with unknown interventions. In *International Conference on Artificial Intelligence and Statistics*, pages 1411–1436. PMLR. [1](#)
- Hasan, U., Hossain, E., and Gani, M. O. (2023). A survey on causal discovery methods for iid and time series data. *Transactions on Machine Learning Research*. [2](#)
- Hoyer, P., Janzing, D., Mooij, J. M., Peters, J., and Schölkopf, B. (2008). Nonlinear causal discovery with additive noise models. *Advances in neural information processing systems*, 21. [5](#)
- Issa, Z., Horvath, B., Lemercier, M., and Salvi, C. (2023). Non-adversarial training of neural sdes with signature kernel scores. *Advances in Neural Information Processing Systems*. [3](#)
- Janzing, D., Balduzzi, D., Grosse-Wentrup, M., and Schölkopf, B. (2013). Quantifying causal influences. *THE ANNALS OF STATISTICS*, pages 2324–2358. [28](#)
- Javier, P. J. E. (2021). causal-ccm a Python implementation of Convergent Cross Mapping. [32](#)
- Ke, N. R., Bilaniuk, O., Goyal, A., Bauer, S., Larochelle, H., Pal, C., and Bengio, Y. (2020). Learning neural causal models from unknown interventions. [1](#)
- Ke, N. R., Chiappa, S., Wang, J. X., Bornschein, J., Goyal, A., Rey, M., Weber, T., Botvinick, M., Mozer, M. C., and Rezende, D. J. (2023). Learning to induce causal structure. In *International Conference on Learning Representations*. [1](#)
- Kim, I., Neykov, M., Balakrishnan, S., and Wasserman, L. (2022). Local permutation tests for conditional independence. *The Annals of Statistics*, 50(6):3388–3414. [5](#)
- Király, F. J. and Oberhauser, H. (2019). Kernels for sequentially ordered data. *Journal of Machine Learning Research*, 20. [3](#)
- Laumann, F., Von Kügelgen, J., Park, J., Schölkopf, B., and Barahona, M. (2023). Kernel-based independence tests for causal structure learning on functional data. *Entropy*, 25(12):1597. [5](#), [9](#), [10](#), [28](#), [30](#), [32](#)
- Lauritzen, S. and Sadeghi, K. (2018). Unifying Markov properties for graphical models. *The Annals of Statistics*, 46(5):2251 – 2278. [25](#)
- Lauritzen, S. L., Dawid, A. P., Larsen, B. N., and Leimer, H.-G. (1990). Independence properties of directed markov fields. *Networks*, 20(5):491–505. [26](#)

- Lawrence, A. R., Kaiser, M., Sampaio, R., and Sipos, M. (2021). Data generating process to evaluate causal discovery techniques for time series data. *arXiv preprint arXiv:2104.08043*. [2](#)
- Lee, S. and Honavar, V. G. (2017). Self-discrepancy conditional independence test. In *Uncertainty in artificial intelligence*, volume 33. [5](#), [9](#), [29](#)
- Lemercier, M., Salvi, C., Damoulas, T., Bonilla, E., and Lyons, T. (2021). Distribution regression for sequential data. In *International Conference on Artificial Intelligence and Statistics*, pages 3754–3762. PMLR. [3](#)
- Li, C. and Fan, X. (2020). On nonparametric conditional independence tests for continuous variables. *Wiley Interdisciplinary Reviews: Computational Statistics*, 12(3):e1489. [4](#)
- Lorch, L., Rothfuss, J., Schölkopf, B., and Krause, A. (2021). Dibs: Differentiable bayesian structure learning. *Advances in Neural Information Processing Systems*, 34:24111–24123. [1](#)
- Lundborg, A. R., Shah, R. D., and Peters, J. (2022). Conditional independence testing in hilbert spaces with applications to functional data analysis. *Journal of the Royal Statistical Society Series B: Statistical Methodology*, 84(5):1821–1850. [5](#)
- Malinsky, D. and Spirtes, P. (2018). Causal structure learning from multivariate time series in settings with unmeasured confounding. In *Proceedings of 2018 ACM SIGKDD workshop on causal discovery*, pages 23–47. PMLR. [5](#)
- Marinazzo, D., Pellicoro, M., and Stramaglia, S. (2008). Kernel method for nonlinear granger causality. *Physical review letters*, 100(14):144103. [5](#)
- Meek, C. (2014). Toward learning graphical and causal process models. In *CI@ UAI*, pages 43–48. [6](#)
- Mogensen, S. W. (2023). Weak equivalence of local independence graphs. *arXiv preprint arXiv:2302.12541*. [2](#)
- Mogensen, S. W. and Hansen, N. R. (2020). Markov equivalence of marginalized local independence graphs. *The Annals of Statistics*, 48(1):539 – 559. [6](#)
- Mogensen, S. W. and Hansen, N. R. (2022). Graphical modeling of stochastic processes driven by correlated noise. *Bernoulli*, 28(4):3023 – 3050. [2](#)
- Mogensen, S. W., Malinsky, D., and Hansen, N. R. (2018). Causal learning for partially observed stochastic dynamical systems. In *Conference on Uncertainty in Artificial Intelligence*, pages 350–360. [6](#)
- Montagna, F., Mastakouri, A. A., Eulig, E., Noceti, N., Rosasco, L., Janzing, D., Aragam, B., and Locatello, F. (2023a). Assumption violations in causal discovery and the robustness of score matching. In *Thirty-seventh Conference on Neural Information Processing Systems*. [1](#)
- Montagna, F., Noceti, N., Rosasco, L., Zhang, K., and Locatello, F. (2023b). Scalable causal discovery with score matching. In van der Schaar, M., Zhang, C., and Janzing, D., editors, *Proceedings of the Second Conference on Causal Learning and Reasoning*, volume 213 of *Proceedings of Machine Learning Research*, pages 752–771. PMLR. [1](#)
- Mooij, J. M., Janzing, D., and Schölkopf, B. (2013). From ordinary differential equations to structural causal models: the deterministic case. In *Proceedings of the Twenty-Ninth Conference on Uncertainty in Artificial Intelligence*, UAI’13, page 440–448, Arlington, Virginia, USA. AUAI Press. [6](#)

- Muandet, K., Fukumizu, K., Sriperumbudur, B., Schölkopf, B., et al. (2017). Kernel mean embedding of distributions: A review and beyond. *Foundations and Trends® in Machine Learning*, 10(1-2):1–141. [4](#)
- Pamfil, R., Sriwattanaworachai, N., Desai, S., Pilgerstorfer, P., Georgatzis, K., Beaumont, P., and Aragam, B. (2020). Dynotears: Structure learning from time-series data. In *International Conference on Artificial Intelligence and Statistics*, pages 1595–1605. PMLR. [5](#)
- Park, J. and Muandet, K. (2020). A measure-theoretic approach to kernel conditional mean embeddings. *Advances in neural information processing systems*, 33:21247–21259. [4](#), [5](#), [27](#)
- Pearl, J. (2009). *Causality*. Cambridge university press. [26](#)
- Peters, J., Bauer, S., and Pfister, N. (2022). Causal models for dynamical systems. In *Probabilistic and Causal Inference: The Works of Judea Pearl*, pages 671–690. Association for Computing Machinery. [2](#), [6](#), [21](#)
- Peters, J., Janzing, D., and Schölkopf, B. (2017). *Elements of causal inference: foundations and learning algorithms*. The MIT Press. [5](#), [7](#), [8](#), [22](#), [23](#)
- Rogers, L. C. G. and Williams, D. (2000). *Diffusions, Markov processes, and martingales. Vol. 2*. Cambridge Mathematical Library. Cambridge University Press, Cambridge. Itô calculus, Reprint of the second (1994) edition. [2](#), [21](#), [23](#), [24](#)
- Rolland, P., Cevher, V., Kleindessner, M., Russell, C., Janzing, D., Schölkopf, B., and Locatello, F. (2022). Score matching enables causal discovery of nonlinear additive noise models. In *International Conference on Machine Learning*, pages 18741–18753. PMLR. [1](#)
- Runge, J. (2018). Causal network reconstruction from time series: From theoretical assumptions to practical estimation. *Chaos: An Interdisciplinary Journal of Nonlinear Science*, 28(7):075310. [5](#)
- Runge, J. (2020). Discovering contemporaneous and lagged causal relations in autocorrelated nonlinear time series datasets. In *Conference on Uncertainty in Artificial Intelligence*, pages 1388–1397. PMLR. [5](#)
- Runge, J., Gerhardus, A., Varando, G., Eyring, V., and Camps-Valls, G. (2023). Causal inference for time series. *Nature Reviews Earth & Environment*, 4(7):487–505. [2](#), [5](#)
- Runge, J., Nowack, P., Kretschmer, M., Flaxman, S., and Sejdinovic, D. (2019). Detecting and quantifying causal associations in large nonlinear time series datasets. *Science advances*, 5(11):eaau4996. [2](#), [5](#), [9](#), [32](#)
- Runge, J., Tibau, X.-A., Bruhns, M., Muñoz-Marí, J., and Camps-Valls, G. (2020). The causality for climate competition. In *NeurIPS 2019 Competition and Demonstration Track*, pages 110–120. PMLR. [5](#)
- Salvi, C., Cass, T., Foster, J., Lyons, T., and Y., W. (2021a). The signature kernel is the solution of a Goursat PDE. *SIAM Journal on Mathematics of Data Science*, 3(3):873–899. [3](#), [4](#)
- Salvi, C., Lemercier, M., Cass, T., Bonilla, E. V., Damoulas, T., and Lyons, T. J. (2021b). Siggpde: Scaling sparse gaussian processes on sequential data. In *International Conference on Machine Learning*, pages 6233–6242. PMLR. [3](#)
- Salvi, C., Lemercier, M., Liu, C., Horvath, B., Damoulas, T., and Lyons, T. (2021c). Higher order kernel mean embeddings to capture filtrations of stochastic processes. *Advances in Neural Information Processing Systems*, 34:16635–16647. [3](#), [8](#)

- Schweder, T. (1970). Composable markov processes. *Journal of applied probability*, 7(2):400–410. [6](#), [22](#)
- Seabold, S. and Perktold, J. (2010). Statsmodels: Econometric and statistical modeling with python. In *Proceedings of the 9th Python in Science Conference*, volume 57, pages 10–25080. Austin, TX. [32](#)
- Sen, R., Suresh, A. T., Shanmugam, K., Dimakis, A. G., and Shakkottai, S. (2017). Model-powered conditional independence test. In Guyon, I., Luxburg, U. V., Bengio, S., Wallach, H., Fergus, R., Vishwanathan, S., and Garnett, R., editors, *Advances in Neural Information Processing Systems*, volume 30. Curran Associates, Inc. [5](#)
- Shah, R. D. and Peters, J. (2020). The hardness of conditional independence testing and the generalised covariance measure. *The Annals of Statistics*, 48(3):1514–1538. [5](#)
- Shojaie, A. and Fox, E. B. (2022). Granger causality: A review and recent advances. *Annual Review of Statistics and Its Application*, 9:289–319. [5](#)
- Singer, H. (1992). Dynamic structural equations in discrete and continuous time. In *Economic Evolution and Demographic Change: Formal Models in Social Sciences*, pages 306–320. Springer. [2](#)
- Sokol, A. and Hansen, N. (2013). Causal interpretation of stochastic differential equations. *Electronic Journal of Probability*, 19. [22](#)
- Spirtes, P., Glymour, C. N., and Scheines, R. (2000). *Causation, prediction, and search*. MIT press. [1](#), [7](#), [23](#)
- Strobl, E. V., Zhang, K., and Visweswaran, S. (2019). Approximate kernel-based conditional independence tests for fast non-parametric causal discovery. *Journal of Causal Inference*, 7(1). [5](#)
- Sugihara, G., May, R., Ye, H., Hsieh, C.-h., Deyle, E., Fogarty, M., and Munch, S. (2012). Detecting causality in complex ecosystems. *science*, 338(6106):496–500. [9](#)
- Székely, G. J., Rizzo, M. L., and Bakirov, N. K. (2007). Measuring and testing dependence by correlation of distances. *Ann. Statist.* 35 (6) 2769 - 2794. [32](#)
- Tsamardinos, I. and Borboudakis, G. (2010). Permutation testing improves bayesian network learning. In *Joint European conference on machine learning and knowledge discovery in databases*, pages 322–337. Springer. [4](#)
- Verma, T. and Pearl, J. (1990). Equivalence and synthesis of causal models. In *Proceedings of the Sixth Annual Conference on Uncertainty in Artificial Intelligence*, UAI '90, page 255–270, USA. Elsevier Science Inc. [23](#), [24](#)
- Vowels, M. J., Camgoz, N. C., and Bowden, R. (2022). D’ya like dags? a survey on structure learning and causal discovery. *ACM Computing Surveys*, 55(4):1–36. [1](#)
- Yu, Y., Chen, J., Gao, T., and Yu, M. (2019). Dag-gnn: Dag structure learning with graph neural networks. In *International Conference on Machine Learning*, pages 7154–7163. PMLR. [1](#)
- Zhang, K., Peters, J., Janzing, D., and Schölkopf, B. (2011). Kernel-based conditional independence test and application in causal discovery. In *Proceedings of the Twenty-Seventh Conference on Uncertainty in Artificial Intelligence*, UAI’11, page 804–813, Arlington, Virginia, USA. AUAI Press. [4](#), [29](#)

- Zhang, Q., Filippi, S., Flaxman, S., and Sejdinovic, D. (2017). Feature-to-feature regression for a two-step conditional independence test. [4](#)
- Zheng, X., Aragam, B., Ravikumar, P. K., and Xing, E. P. (2018). Dags with no tears: Continuous optimization for structure learning. *Advances in neural information processing systems*, 31. [1](#)
- Zheng, X., Dan, C., Aragam, B., Ravikumar, P., and Xing, E. (2020). Learning sparse nonparametric dags. In *International Conference on Artificial Intelligence and Statistics*, pages 3414–3425. PMLR. [1](#)

A Proofs and theoretical digressions

A.1 Intuition and Details for the SDE Model

Making the actual dependence of μ^k and σ^k on their arguments in eq. (1) explicit, we can rewrite it as

$$\begin{cases} dX_t^k = \mu^k(X_{[0,t]}^{\text{pa}_k})dt + \sigma^k(X_{[0,t]}^{\text{pa}_k})dW_t^k, \\ X_0^k = x_0^k \quad k \in [d]. \end{cases} \quad (6)$$

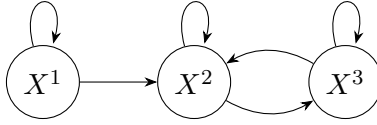
Then μ^k, σ^k are functions defined on $C([0, +\infty), \mathbb{R}^{\dim(\text{pa}_k)})$ (or some suitable subspace thereof): Lipschitz conditions on the coefficients that guarantee existence and uniqueness for this type of SDE can be found in [Rogers and Williams \(2000\)](#), which we assume to hold throughout. Each W^k is an m_k -dimensional Brownian motion (a collection of m_k independent 1-dimensional Brownian motions, that is), σ^k maps to the space of $n_k \times m_k$ -dimensional matrices, and the noises W^k together with the (possibly random) initial conditions x_0^k are jointly independent. In other words, the system can be written as an $n := n_1 + \dots + n_d$ -dimensional SDE driven by an $m := m_1 + \dots + m_d$ -dimensional Brownian motion, with a block-diagonal diffusion coefficient σ (since the noise is unobserved, this structure has to be imposed if we wish not to deal with unobserved confounding). The superscript pa_k refers to the parents of the k^{th} node in \mathcal{G} , which may (and most often does) contain k itself. Intuitively, all of this means that, for all times t and small increments Δt , the increment of the solution $X_{t+\Delta t}^k - X_t^k$ is random with distribution that is well-approximated by a multivariate normal with mean $\mu^k(X_{[0,t]}^{\text{pa}_k})\Delta t$ and covariance function $\sigma^k(X_{[0,t]}^{\text{pa}_k})\sigma^k(X_{[0,t]}^{\text{pa}_k})^\top \Delta t$, and independent of the history of the system up to time t . This interpretation can actually be made precise by showing that these piecewise constant paths converge in law to the true solution (usually known as the weak solution, when viewed in this way).

We will refer to \mathcal{G} as the *dependency graph* of the eq. (1), which we refer to as the *SDE model* for brevity. Compared to that of [Peters et al. \(2022\)](#), this model is slightly more general in that (i) it allows for path-dependency and (ii) for each node to represent a multidimensional process; the special case of state-dependent SDE—i.e., in which μ and σ only depend on X_t , the value of X at time t —continues to be an important special case, although our model also accommodates delayed SDEs (the coefficients depend on the value of X at a prior instant in time, e.g., $X_{t-\tau}$ for fixed or possibly random/time-dependent $\tau > 0$), and SDEs that depend on quantities involving the whole past of X , such as the average $t^{-1} \int_0^t X_s ds$. We note that the choice not to make the coefficients explicitly time-dependent is deliberate and motivated by the requirement that the system be *causally stationary* (the causal relations between the variables do not change over time).

Given that we are considering the dynamic setting, it is generally natural to allow for \mathcal{G} to have cycles. This comes at no additional requirement of consistency constraints as it does in the static case (see for example [Bongers et al. \(2021\)](#)), since the causal arrows in the model eq. (1) should be thought of as ‘pointing towards the infinitesimal future, with infinitesimal magnitude’, integrated over the whole time interval considered. Indeed, the system of SDEs does not require any global consistency to be well-posed, other than the regularity and growth conditions that guarantee global-in-time existence and uniqueness. On the other hand, we will be interested in the potential for constraint-based causal discovery of such systems, qualified by the following assumption on the types of conditional independencies that we allow to be tested in continuous time:

A.2 Counterexample for Cyclic Causal Discovery in the SDE Model

We restate our example, namely that the oracle in Assumption 3.1 is not powerful enough to rule out a directed edge $X^1 \rightarrow X^3$ for an SDE model with the following dependency graph:



Testing $X_{[0,s]}^1 \perp\!\!\!\perp X_{[s,s+h]}^3 \mid X_{[0,s]}^{2,3}$, will not remove the edge, due to the open path

$$X_{[0,s]}^1 \rightarrow X_{[s,s+h]}^1 \rightarrow X_{[s,s+h]}^2 \rightarrow X_{[s,s+h]}^3.$$

Testing $X_{[0,s]}^1 \perp\!\!\!\perp X_{[s,s+h]}^3 \mid X_{[0,s]}^3, X_{[0,s+h]}^2$, on the other hand, runs into the collider

$$X_{[0,s]}^1 \rightarrow X_{[s,s+h]}^1 \rightarrow X_{[s,s+h]}^2 \leftarrow X_{[s,s+h]}^3.$$

There is no other way of splitting up the time interval (even allowing for more than 2 subintervals) that overcomes both these problems: when testing $X_{[0,s]}^1 \perp\!\!\!\perp X_{[s,s+h]}^3$ (as is necessary in order to rely on time to obtain direction of the arrow), if X^2 is not conditioned on over $[s, s+h]$ it will be a mediator, and if it is, it will be a collider.

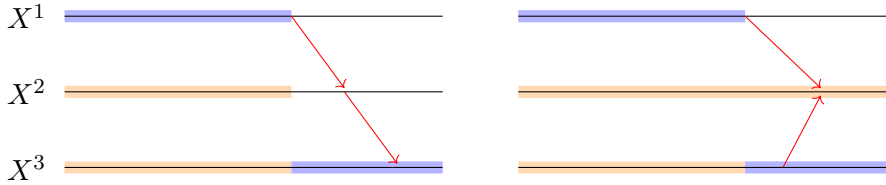


Figure 4: The blue highlighter is for intervals over which the path is being tested for independence, while orange is for conditioning. The first figure illustrates the path opened by the unconditioned-on mediator $X_{[s,s+h]}^2$, while the second illustrates the path opened by the same variable acting as a conditioned-on collider. While not quite possible to draw figures this way, it is helpful to think of the arrows as pointing from values to increments $X_t \rightarrow (Y_{t+dt} - Y_t)$, infinitesimally, with the total causal effect accrued over time.

What would be needed to detect the edge in the above example (and to perform causal discovery more generally in the cyclic case), is the availability of tests of *strong instantaneous non-causality in the Granger sense* as defined in [Florens and Fougere \(1996\)](#). This reflects the fact that the SDE model is ‘acyclic at infinitesimal scales’. Unfortunately, such a property—which has to do with the Doob-Meyer decompositions of functions of the process w.r.t. two different filtrations—is much more difficult to test for, as it is infinitesimal in nature. Recent progress in this direction was made in [Christgau et al. \(2023\)](#) for the case of SDEs driven by jump processes; this local independence criterion, which goes back to [Schweder \(1970\)](#), is however *weak* in the sense that it only takes into account the Doob-Meyer decomposition of X and not functions of it, and is not therefore able, for example, to detect dependence in the diffusion coefficient [Gégout-Petit and Commenges \(2010\)](#). Here we take the view that a continuously-indexed path, queried over an interval, can be considered as an observational distribution (cf. the discussion in [Sokol and Hansen \(2013\)](#) on whether the infinitesimal generator can be considered ‘observational’).

A.3 Proof of Proposition 3.3

Proof of Proposition 3.3. Since \mathcal{G} is acyclic, a directed cycle in $\tilde{\mathcal{G}}$ that is not a loop must contain nodes both in V_0, V_1 . But there can be no such directed cycles, since edges only travel in the direction $V_0 \rightarrow V_1$, by construction of $\tilde{\mathcal{G}}$. Since $\tilde{\mathcal{G}}$ also free of loops, it is a DAG. We now show that there exists an SCM over $\tilde{\mathcal{G}}$ with the path-valued random variables of the statement: Markovianity will then follow from [Peters et al. \(2017, Proposition 6.31\)](#), original

to [Verma and Pearl \(1990\)](#). In other words, we must show there exist Borel-measurable functions (setting $t := s + h$)

$$F_0^k: \mathbb{R}^{\dim(\text{pa}_k)} \times C([0, s], \mathbb{R}^{m_k}) \times C([0, s], \mathbb{R}^{\dim(\text{pa}_k \setminus \{k\})}) \rightarrow C([0, s], \mathbb{R}^{n_k})$$

$$(x_0^{\text{pa}(k)}, W_{[0,s]}^k; X_{[0,s]}^{\text{pa}_k \setminus \{k\}}) \mapsto X_{[0,s]}^k$$

and

$$F_1^k: C([s, t], \mathbb{R}^{m_k}) \times C([0, s], \mathbb{R}^{\dim(\text{pa}_k)}) \times C([s, t], \mathbb{R}^{\dim(\text{pa}_k \setminus \{k\})}) \rightarrow C([0, s], \mathbb{R}^{n_k})$$

$$(W_{[s,t]}^k; X_{[0,s]}^{\text{pa}_k}, X_{[s,t]}^{\text{pa}_k \setminus \{k\}}) \mapsto X_{[0,s]}^k$$

with the initial conditions x^0 and Brownian path segments $W_{[0,s]}^k, W_{[s,t]}^k$ collectively independent. This independence follows from the definition of the SDE model and from independence of Brownian increments over disjoint or consecutive intervals. These functions are partial in that they are not defined on the whole space of continuous functions on the interval: we only need to show them to be defined on a measurable set of paths that contains all solutions of SDEs on the required interval. F_1^k is defined as follows, with care to make explicit the dependence on the solution on the two intervals via the operation of path-concatenation $*$:

$$F_1^k(X_{[s,t]}^k) = \text{solution of } X_u^k = X_s^k + \int_0^u \mu^k(X_{[0,s]}^{\text{pa}_k \setminus \{k\}} * X_{[s,u]}^{\text{pa}_k \setminus \{k\}}, X_{[0,s]}^k * X_{[s,u]}^k) dt$$

$$+ \sigma^k(X_{[0,s]}^{\text{pa}_k \setminus \{k\}} * X_{[s,u]}^{\text{pa}_k \setminus \{k\}}, X_{[0,s]}^k * X_{[s,u]}^k) dW_t^k$$

We have also separated out the k -th component of the solution from the rest of the arguments on which σ^k, μ^k are dependent, which we consider part of the measurable adapted dependence on $W^{\text{pa} \setminus \{k\}}$ needed in the existence and uniqueness theorem. F_0^k is defined similarly (with no dependence on past path-segments and with x_0^k replacing X_s^k). Such functions are well-known to be well-defined and measurable [Rogers and Williams \(2000, Theorem 10.4\)](#). \square

A.4 Faithfulness and causal minimality

We proceed with a brief and informal discussion of causal minimality and faithfulness, a notably delicate topic even in the case of standard SCMs. We remain in our setting of acyclicity + loops. It is not difficult to convert the classical counterexamples of faithfulness (Example 6.34 in [Peters et al. \(2017\)](#)) into ones for our SDE model. It is also reasonable to conjecture, following Theorem 3.2 in [Spirtes et al. \(2000\)](#) that, allowing for the diffusion coefficients σ to range in some ‘reasonable’ finite-dimensional family (such as linear or affine functions) and drawing the parameters of such family from a distribution which has positive density w.r.t. the Lebesgue measure (and independently of the noise), the resulting distribution on path-space, split over $[0, s]$ and $[s, t]$, will be a.s. faithful, for any $0 < s < t$ w.r.t. the lifted dependency graph. We do not attempt a proof of such statement here, which might require quite some effort and technique. Causal minimality, on the other hand, is generally easier to understand and can be expected to hold for the arrow $X_{[0,s]}^i \rightarrow X_{[s,t]}^j$ whenever the following condition is satisfied: the conditional distribution $X_u^j | X^{\text{pa}_j \setminus \{i\}} = x^j$ admits a positive density on some submanifold M_u^x of \mathbb{R}^n and for all u there exist $x_1^i, x_2^i \in M_u^x, x_1^i \neq x_2^i$, s.t. $(\mu^j, \sigma^j)(x, x_1^i) \neq (\mu^j, \sigma^j)(x, x_2^i)$.

Example A.1 (Causal minimality). The fact that we are allowing for variables to have more than one dimension means the causal minimality condition is not a trivial one, as the following examples demonstrate. Let $X^1 = (W, 0)$ where W is a 1-dimensional Brownian motion (so that $n_1 = 2$), and let μ^2 and/or σ^2 depend on X^1 only through its second coordinate. Then, even though this dependence may be non-trivial, causal minimality does not hold. This may lead one to believe that one can generically only expect causal minimality to hold if $m = n$, but this is not the case. Take, for example, $d = 4 = n$ and assume $\sigma^3 \equiv 0$, i.e., X^3 has

no driving Brownian motion, so that m is only 3. Assume, furthermore, that $\text{pa}_4 = \{4\}$. Then, by Hörmander’s Lie bracket-generating condition (see for example §V.38 in [Rogers and Williams \(2000\)](#)), (X^1, X^2, X^3) has a density in \mathbb{R}^3 for any choice of an initial condition, if $(\sigma^1(x), 0, 0), (0, \sigma^2(x), 0)$ span \mathbb{R}^2 for all $x \in \mathbb{R}^3$ and $[(\sigma^1(x), 0, 0), \mu] = \sigma^1 \partial_1 \mu - \mu^i \partial_i \sigma^1$ or $[(\sigma^2(x), 0, 0), \mu]$ span the third direction. Arrows going from the first three nodes to the fourth will be necessary for Markovianity as long as the coefficients of X^4 depend on the respective variables on the support of such density. The point is that even though (X^1, X^2, X^3) is only driven by a two-dimensional Brownian motion, the coefficients of the SDE (at the initial condition) impart a ‘twist’ to the solution, making causal minimality a trivial condition on (σ^4, μ^4) which is verified as soon as there is any dependency.

A.5 Proof of Corollary 3.7

Proof. This is clear from the data generating mechanism in eq. (1) where all Brownian motions dW_t^k and initial conditions X_0^k are jointly independent. Since $X_{[0,T]}^j$ is fully determined by $\{X_0^{\text{an}_j}, dW_t^{\text{an}_j}\}$ where an_j are the ancestors of j in \mathcal{G} , it follows that $i \in \text{an}_j$ if and only if $X_{[0,T]}^j \not\perp X_0^i$. Since we already know from the CPDAG that i and j are adjacent and the graph is acyclic, $i \in \text{an}_j$ implies $i \rightarrow j$. \square

A.6 Proof of Theorem 3.4

Proof of Theorem 3.4. We begin with proving correctness of the recovery of the skeleton modulo loops. This will follow if we show that for $(i \rightarrow j) \notin \mathcal{G}$ for $i, j \in V$ distinct

$$i_0 \perp_{\tilde{\mathcal{G}}} j_1 \mid \{j_0\} \cup \{k_0, k_1 \mid k \in \text{pa}_j^{\mathcal{G}} \setminus \{j\}\},$$

where $\perp_{\tilde{\mathcal{G}}}$ denotes d -separation in the graph $\tilde{\mathcal{G}}$. Indeed, eventually, the set K in the algorithm will take the value $\{k_0, k_1 \mid k \in \text{pa}_j^{\mathcal{G}} \setminus \{j\}\}$, at which point the three edges $i_0 \rightarrow j_0, i_1 \rightarrow j_1, i_0 \rightarrow j_1$ (which are either all present or all absent, inductively, by construction of \tilde{E}) are deleted. (Of course it may be that these edges are deleted before this, if a smaller or different d -separating set is found, but note that edges are never added.) All undirected paths between i_0 and j_1 factor as $i_0 \cdots h_0 \rightarrow l_1 \cdots j_1$, where the dots stand for a possibly empty undirected path. All such paths with $l_1 = j$ are blocked by $\{j_0\} \cup \{k_0 \mid k \in \text{pa}_j^{\mathcal{G}} \setminus \{j\}\}$, so we focus our attention on the case in which $l_1 \cdots j_1$ is non-empty. Here we follow a similar argument to that of [Verma and Pearl \(1990, Lemma 1\)](#). If $l_1 \cdots j_1$ is of the form $l_1^1 \cdots l_1^r \rightarrow j_1$ (with $l_1^1 = l_1$) it is blocked by $\{k_1 \mid k \in \text{pa}_j^{\mathcal{G}} \setminus \{j\}\}$. Assume instead it is of the form $l_1^1 \cdots l_1^r \leftarrow j_1$ and let $1 \leq q \leq r$ be such that l_1^q is the first collider on the entire path $i_0 \cdots j_1$, starting from j_1 and travelling back: certainly this exists (and belongs to V_1), thanks to the arrows $h_0 \rightarrow l_1^1$ and $l_1^r \leftarrow j_1$. For the path $i_0 \cdots j_1$ to be open given the conditioning set, it must be the case that l_1^p must be an ancestor (in $\tilde{\mathcal{G}}$) or member of $\{k_1 \mid k \in \text{pa}_j^{\mathcal{G}} \setminus \{j\}\}$ (l_1^p cannot be an ancestor of nodes in V_0): this would yield a directed cycle, which is impossible.

We argue similarly for the loop-removal phase. If $(i \rightarrow i) \notin \mathcal{G} \iff (i_0 \rightarrow i_1) \notin \tilde{\mathcal{G}}$, we must show

$$i_0 \perp_{\tilde{\mathcal{G}}} i_1 \mid \{k_0, k_1 \mid k \in \text{pa}_i^{\mathcal{G}} \setminus \{i\}\}$$

Consider a path $i_0 \cdots h_0 \rightarrow l_1 \cdots i_1$ in $\tilde{\mathcal{G}}$. If the segment $l_1 \cdots i_1$ is non-empty we conclude that the path is blocked by the same argument as above (with i_1 replacing j_1). Assume that the path is of the form $i_0 \cdots h_0 \rightarrow i_1$ (with $i_0 \neq h_0$ since $(i_0 \rightarrow i_1) \notin \tilde{E}$): in this case $h \in \text{pa}_i^{\mathcal{G}} \setminus \{i\}$ and the path is again blocked. Thus all paths are blocked and the proof is complete. \square

A.7 Global Markov Property for the Symmetric Independence Criterion

In this section, we provide a proof for the global Markov property of the symmetric independence criterion in order for the PC-algorithm to be applicable. It is based on the notion of independence models:

Definition A.2. Let $V \cong \{1, \dots, n\}$ be a set. An *independence model* $\mathcal{J}(V)$ over V is a ternary relation over disjoint subsets of V ,

$$\mathcal{J}(V) \subset \{(A, B, C) \mid A, B, C \subset V \text{ disjoint}\}$$

When (A, B, C) is a triple in $\mathcal{J}(V)$, $(A, B, C) \in \mathcal{J}(V)$, we also use $\langle A, B \mid C \rangle$ to denote (A, B, C) . This notation highlights the fact that C is a conditioning set. An independence model $\mathcal{J}(V)$ is called a *semigraphoid* if 1.-4. hold for all disjoint $A, B, C \subset V$.

1. (symmetry) $\langle A, B \mid C \rangle \in \mathcal{J}(V) \Rightarrow \langle B, A \mid C \rangle \in \mathcal{J}(V)$
2. (decomposition) $\langle A, B \mid C \rangle \in \mathcal{J}(V)$ and $D \subset B \Rightarrow \langle A, D \mid C \rangle \in \mathcal{J}(V)$
3. (weak union) $\langle A, B \cup D \mid C \rangle \in \mathcal{J}(V) \Rightarrow \langle A, B \mid C \cup D \rangle \in \mathcal{J}(V)$
4. (contraction) $\langle A, B \mid C \rangle \in \mathcal{J}(V)$ and $\langle A, D \mid B \cup C \rangle \in \mathcal{J}(V) \Rightarrow \langle A, B \cup D \mid C \rangle \in \mathcal{J}(V)$

A semigraphoid $\mathcal{J}(V)$ is called *graphoid* if 5. holds.

5. (intersection) $\langle A, B \mid C \cup D \rangle \in \mathcal{J}(V)$ and $\langle A, D \mid B \cup C \rangle \in \mathcal{J}(V) \Rightarrow \langle A, B \cup D \mid C \rangle \in \mathcal{J}(V)$

An independence model $\mathcal{J}(V)$ called *compositional* if 6. holds.

6. (composition) $\langle A, B \mid C \rangle \in \mathcal{J}(V)$ and $\langle A, D \mid C \rangle \in \mathcal{J}(V) \Rightarrow \langle A, B \cup D \mid C \rangle \in \mathcal{J}(V)$

The graphical criterion of d-separation defines an independence model on a DAG $\mathcal{G} = (V, \mathcal{E})$ by

$$\mathcal{J}_{d\text{-sep}}(\mathcal{G}) = \{(A, B, C) \mid A, B, C \subset V \text{ disjoint}, A \perp_{d\text{-sep}} B \mid C\} \quad (7)$$

Theorem A.3 (Lauritzen and Sadeghi (2018)). *For any DAG $\mathcal{G} = (V, \mathcal{E})$, the independence model $\mathcal{J}_{d\text{-sep}}(\mathcal{G})$ is a compositional graphoid.*

Let $V = \{1, \dots, n\}$. Given random variables $X^i : (\Omega, \mathcal{A}, P) \rightarrow (\mathcal{X}^i, \mathcal{A}_i)$, $i \in V$, and $A, B, C \subset V$ disjoint, conditional independence

$$X^A \perp_P X^B \mid X^C :\Leftrightarrow \sigma(X^A) \perp_P \sigma(X^B) \mid \sigma(X^C)$$

defines the *probabilistic independence model*

$$\mathcal{J}(P) = \{(A, B, C) \mid A, B, C \subset V \text{ disjoint}, X_A \perp_P X_B \mid X_C\}. \quad (8)$$

We will use this as a *symmetric conditional independence* relation. Note that X^i may take values in a path-space in which case it is a stochastic process. The independence model $\mathcal{J}(P)$ is a semigraphoid which is an immediate consequence of sub- σ -algebra properties.

For $v \in V$, we let nd_v denote the set of *nondescendants* of v , i.e., the set of nodes i such that there is no directed path from v to i .

Definition A.4 (Directed global and local Markov properties). Let $\mathcal{G} = (V, \mathcal{E})$ be a DAG and $\mathcal{J}(V)$ be an independence model over V . The independence model $\mathcal{J}(V)$ satisfies the *global Markov property w.r.t. \mathcal{G}* $:\Leftrightarrow$

$$\langle A, B \mid C \rangle \in \mathcal{J}_{d\text{-sep}}(\mathcal{G}) \quad \Rightarrow \quad \langle A, B \mid C \rangle \in \mathcal{J}(V) \quad \forall A, B, C \subset V \text{ disjoint} \quad (9)$$

The independence model $\mathcal{J}(V)$ satisfies the *directed local Markov property w.r.t. \mathcal{G}* $:\Leftrightarrow$

$$\langle \{v\}, (\text{nd}_v \setminus \text{pa}_v) \mid \text{pa}_v \rangle \in \mathcal{J}(V) \text{ for all } v \in V \quad (10)$$

Theorem A.5 (Lauritzen et al. (1990)). Let $\mathcal{G} = (V, \mathcal{E})$ be a DAG, let and $\mathcal{J}(V)$ a semi-graphoid over V . The directed global and local Markov properties are equivalent, that is,

$$\mathcal{J}(V) \text{ satisfies eq. (9) w.r.t. } \mathcal{G} \Leftrightarrow \mathcal{J}(V) \text{ satisfies eq. (10) w.r.t. } \mathcal{G} \quad (11)$$

We therefore only have to establish the local Markov property for the symmetric independence model $\perp\!\!\!\perp_{\text{sym}}$:

Proposition A.6. Let X be a set of variables induces by the model in eq. (6) with a constant and diagonal diffusion matrix s.t. it induces the DAG $\mathcal{G} = (V, \mathcal{E})$. Then the system satisfies the directed local Markov property w.r.t \mathcal{G} ,

$$X^i \perp\!\!\!\perp_{\text{sym}} \text{nd}_{X^i} \setminus \text{pa}_{X^i} \mid \text{pa}_{X^i} \quad \forall i \in \{1, \dots, n\} \quad (12)$$

Proof. The idea of the proof is that all information about node X_i is contained in its parents $\text{pa}_i := \text{pa}_{X^i}$, the Brownian motion W_i , and the initial condition X_0^i . A similar idea can be used to show the result in the case of a SCM Pearl (2009). We let $\tilde{\mathcal{J}}(P)$ denote the semigraphoid induced by $\perp\!\!\!\perp_{\text{sym}}$ on the variable set $\tilde{V} = \{X^1, \dots, X^n\} \cup \{W^1, \dots, W^n\} \cup \{X_0^1, \dots, X_0^n\}$, and we let $\mathcal{J}(P)$ denote the semigraphoid induced by $\perp\!\!\!\perp_{\text{sym}}$ on the variable set $V = \{X^1, \dots, X^n\}$. We define the DAG

$$\tilde{\mathcal{G}} = \left(\tilde{V} = \{X^1, \dots, X^n\} \cup \{W^1, \dots, W^n\} \cup \{X_0^1, \dots, X_0^n\}, \tilde{\mathcal{E}} = \mathcal{E} \cup \{X^j \leftarrow W^j\} \cup \{X^j \leftarrow X_0^j\} \right). \quad (13)$$

By construction, $\mathcal{F}_t(X^i) \subset \mathcal{F}_t(W^i) \vee \mathcal{F}_t(X^{\text{pa}_i}) \vee \sigma(X_0^i)$, and therefore

$$\mathcal{F}_t(X^i) \perp\!\!\!\perp \mathcal{F}_t(X^{\text{nd}_i \setminus \text{pa}_i} \vee W^{-i} \vee X_0^{-i}) \mid \mathcal{F}_t(X^{\text{pa}_i}) \vee \mathcal{F}_t(W^i) \vee \sigma(X_0^i)$$

where the parent and nondescendant sets are to be read in the graph \mathcal{G} , $W^{-i} = \{W_1, \dots, W_n\} \setminus \{W_i\}$, and $X_0^{-i} = \{X_0^1, \dots, X_0^n\} \setminus \{X_0^i\}$. The above statement corresponds to eq. (10) when $v \in \{X_1, \dots, X_n\}$. When $v = W_i$ or $v = X_0^i$, v has no parents in $\tilde{\mathcal{G}}$ and eq. (10) also holds. Therefore, the independence model $\tilde{\mathcal{J}}(P)$ satisfies the local directed Markov property w.r.t. to $\tilde{\mathcal{G}}$.

The independence model $\tilde{\mathcal{J}}(P)$ is a semigraphoid, and by Theorem A.5 it satisfies eq. (9) w.r.t. $\tilde{\mathcal{G}}$. We have $X^i \perp\!\!\!\perp_{d\text{-sep}} X^{\text{nd}_i \setminus \text{pa}_i} \mid X^{\text{pa}_i}$ in $\tilde{\mathcal{G}}$, and one therefore has

$$\mathcal{F}_t(X^i) \perp\!\!\!\perp \mathcal{F}_t(X^{\text{nd}_i \setminus \text{pa}_i}) \mid \mathcal{F}_t(X^{\text{pa}_i})$$

establishing eq. (10) for $\mathcal{J}(P)$ w.r.t. \mathcal{G} . □

A.8 Consistency of the conditional independence test

In this section, we argue, that under certain assumptions on our system, Theorem 1 of Doran et al. (2014) still holds even without assuming the existence of a density. At first, it is to be noted that the signature kernel (2) is bounded on compact sets $C \subset \text{BV}(\mathcal{C}^0(I, \mathbb{R}^{d_x}))$ of BV paths, an assumption that can be made as we evaluate our SDEs over finite, discrete time steps. Satisfying this boundedness, it defines an RKHS over these compact sets. In addition, the signature kernel is characteristic on these bounded sets (see Proposition 3.3 Cass et al. (2023)). We use the notation $X : (\Omega, \mathcal{A}, P) \rightarrow (\mathcal{X}, \mathcal{A}_X)$, $Y : (\Omega, \mathcal{A}, P) \rightarrow (\mathcal{Y}, \mathcal{A}_Y)$, $Z : (\Omega, \mathcal{A}, P) \rightarrow (\mathcal{Z}, \mathcal{A}_Z)$ with $cX, \mathcal{Y}, \mathcal{Z}$ being compact subsets in $\text{BV}(\mathcal{C}^0(I, \mathbb{R}^{d_x}))$, $\text{BV}(\mathcal{C}^0(I, \mathbb{R}^{d_y}))$, $\text{BV}(\mathcal{C}^0(I, \mathbb{R}^{d_z}))$ and denote the RKHS's defined by the signature kernel as (\mathcal{H}_X, k_X) , (\mathcal{H}_Y, k_Y) , (\mathcal{H}_Z, k_Z) .

Our measure-theoretical argumentation now follows the definitions in [Park and Muandet \(2020\)](#) and the original proof in [Doran et al. \(2014\)](#). Let \mathcal{H} be a Banach space, $\mathcal{E} \subset \mathcal{F}$ a sub- σ -algebra of the Borel- σ -algebra.

Definition A.7. Let $H : (\Omega, \mathcal{A}, P) \rightarrow (\mathcal{H}, \mathcal{F})$ a Bochner P -integrable random variable. The *conditional expectation of H w.r.t \mathcal{E}* is a Bochner P -integrable RV $H' : (\Omega, \mathcal{A}, P) \rightarrow (\mathcal{H}, \mathcal{E})$ such that

$$\forall A \in \mathcal{E} \quad \int_A H dP = \int_A H' dP.$$

Due to the existence and (almost sure) uniqueness, such an H' is denoted $\mathbb{E}[H \mid \mathcal{E}]$ with the notation $\mathbb{E}[H \mid Z] := \mathbb{E}[H \mid \sigma(Z)]$ for a general $Z : (\Omega, \mathcal{A}, P) \rightarrow (\mathcal{Z}, \mathcal{A}_Z)$ which in turn can be used to define the *conditional expectation* $P(A \mid \mathcal{E}) := \mathbb{E}[\mathbb{1}_A \mid \mathcal{E}]$ and can be used to define the *conditional kernel mean embedding*

$$\mu_{X|Z} := \mu_{P_{X|Z}} := \mathbb{E}_{X|Z}[k_{\mathcal{X}}(X, \cdot) \mid Z]$$

As proven in Theorem 5.8 of [Park and Muandet \(2020\)](#) under the assumption, that $P_{X|Z} := \mathbb{E}[\cdot, \mid Z]$ admits a regular version (meaning its can be written as a transition kernel, see [Park and Muandet \(2020\)](#)) and $k_{\mathcal{X}} \otimes k_{\mathcal{Y}}$ is characteristic, it holds that

$$X \perp\!\!\!\perp Y \mid Z \Leftrightarrow \|\mu_{XY|Z} - \mu_{X|Z} \otimes \mu_{Y|Z}\|_{\mathcal{H}_{\mathcal{X}} \otimes \mathcal{H}_{\mathcal{Y}}} = 0 \Leftrightarrow \|\mu_{XY|Z} \otimes \mu_Z - \mu_{X|Z} \otimes \mu_{Y|Z} \otimes \mu_Z\|_{\mathcal{H}_{\mathcal{X}} \otimes \mathcal{H}_{\mathcal{Y}} \otimes \mathcal{H}_{\mathcal{Z}}} = 0$$

where the second equivalence is trivial. Let now $\sigma \in \mathcal{S}_n$ be a permutation such that its permutation matrix $M_{\sigma} = (m_{ij})$

$$m_{ij} = \begin{cases} 1 & \text{if } j = \sigma(i), \\ 0 & \text{if } j \neq \sigma(i). \end{cases}$$

satisfies $\text{Tr}(M_{\sigma}) = 0$. The empirical estimates for the given sample $\{(x_i, y_i, z_i)\}_{i \in [n]}$ and its permuted version under σ

$$\hat{\mu}_{P_{X,Y,Z}} := \frac{1}{n} \sum_{i=1}^n k_{\mathcal{X}}(x_i, \cdot) \otimes k_{\mathcal{Y}}(y_i, \cdot) \otimes k_{\mathcal{Z}}(z_i, \cdot), \quad (14)$$

$$\hat{\mu}_{P'_{X,Y,Z}} := \frac{1}{n} \sum_{i=1}^n k_{\mathcal{X}}(x_i, \cdot) \otimes k_{\mathcal{Y}}(y_{\sigma(i)}, \cdot) \otimes k_{\mathcal{Z}}(z_i, \cdot). \quad (15)$$

We can now write the distance between test statistic and the approximated test statistic in terms of the sum of the distance between the empirical estimates and its respective counterparts by using the inverse and the regular triangle inequality

$$\begin{aligned} & \left| \|\mu_{XY|Z} \otimes \mu_Z - \mu_{X|Z} \otimes \mu_{Y|Z} \otimes \mu_Z\|_{\mathcal{H}_{\mathcal{X}} \otimes \mathcal{H}_{\mathcal{Y}} \otimes \mathcal{H}_{\mathcal{Z}}} - \|\hat{\mu}_{P_{X,Y,Z}} - \hat{\mu}_{P'_{X,Y,Z}}\|_{\mathcal{H}_{\mathcal{X}} \otimes \mathcal{H}_{\mathcal{Y}} \otimes \mathcal{H}_{\mathcal{Z}}} \right| \\ & \leq \left| \|\mu_{XY|Z} \otimes \mu_Z - \mu_{X|Z} \otimes \mu_{Y|Z} \otimes \mu_Z - \hat{\mu}_{P_{X,Y,Z}} + \hat{\mu}_{P'_{X,Y,Z}}\|_{\mathcal{H}_{\mathcal{X}} \otimes \mathcal{H}_{\mathcal{Y}} \otimes \mathcal{H}_{\mathcal{Z}}} \right| \\ & \leq \|\mu_{XY|Z} \otimes \mu_Z - \hat{\mu}_{P_{X,Y,Z}}\|_{\mathcal{H}_{\mathcal{X}} \otimes \mathcal{H}_{\mathcal{Y}} \otimes \mathcal{H}_{\mathcal{Z}}} + \|\mu_{X|Z} \otimes \mu_{Y|Z} \otimes \mu_Z - \hat{\mu}_{P'_{X,Y,Z}}\|_{\mathcal{H}_{\mathcal{X}} \otimes \mathcal{H}_{\mathcal{Y}} \otimes \mathcal{H}_{\mathcal{Z}}}. \end{aligned}$$

By [Park and Muandet \(2020\)](#), the first term tends to zero for $n \rightarrow \infty$. With a similar line of argumentation as in [Doran et al. \(2014\)](#) on can establish a majorant for the estimated HSCIC,

namely

$$\begin{aligned}
& \|\hat{\mu}_{P_{X,Y,Z}} - \hat{\mu}_{P'_{X,Y,Z}}\|_{\mathcal{H}_X \otimes \mathcal{H}_Y \otimes \mathcal{H}_Z} \\
&= \left\| \frac{1}{n} \sum_{i=1}^n k_X(x_i, \cdot) \otimes k_Y(y_i, \cdot) \otimes k_Z(z_i, \cdot) - \frac{1}{n} \sum_{i=1}^n k_X(x_i, \cdot) \otimes k_Y(y_{\sigma(i)}, \cdot) \otimes k_Z(z_i, \cdot) \right\|_{\mathcal{H}_X \otimes \mathcal{H}_Y \otimes \mathcal{H}_Z} \\
&= \left\| \frac{1}{n} \sum_{i=1}^n k_X(x_i, \cdot) \otimes k_Y(y_i, \cdot) \otimes k_Z(z_i, \cdot) - \frac{1}{n} \sum_{i=\sigma(j), j=1}^n k_X(x_{\sigma^{-1}(i)}, \cdot) \otimes k_Y(y_i, \cdot) \otimes k_Z(z_{\sigma^{-1}(i)}, \cdot) \right\|_{\mathcal{H}_X \otimes \mathcal{H}_Y \otimes \mathcal{H}_Z} \\
&\leq \frac{1}{n} \sum_{i=1}^n \left\| (k_X(x_i, \cdot) - k_X(x_{\sigma^{-1}(i)}, \cdot)) \otimes k_Y(y_i, \cdot) \otimes (k_Z(z_i, \cdot) - k_Z(z_{\sigma^{-1}(i)}, \cdot)) \right\|_{\mathcal{H}_X \otimes \mathcal{H}_Y \otimes \mathcal{H}_Z} \\
&\leq \frac{1}{n} \sum_{i=1}^n \underbrace{\|k_X(x_i, \cdot) - k_X(x_{\sigma^{-1}(i)}, \cdot)\|_{\mathcal{H}_X}}_{\leq 2M_x} \underbrace{\|k_Y(y_i, \cdot)\|_{\mathcal{H}_Y}}_{\leq M_y} \|k_Z(z_i, \cdot) - k_Z(z_{\sigma^{-1}(i)}, \cdot)\|_{\mathcal{H}_Z} \\
&\leq 2M_x M_y \left(\frac{1}{n} \text{Tr}(PD^{RKHS}) \right)
\end{aligned}$$

where the assumptions can be made due to the boundedness of the kernels. Hence, under the assumption that

$$\frac{1}{n} \sum_{i=1}^n \delta_{(x_i, y_{\sigma(i)}, z_i)} \rightarrow P_{X|Z} \otimes P_{Y|Z} \otimes P_Z \quad (16)$$

a statement that holds true in the case of densities (see supplementary material of [Janzing et al. \(2013\)](#)), since $P_{|Z}$ is regular, $\hat{\mu}_{P'_{X,Y,Z}} \rightarrow \mu_{X|Z} \otimes \mu_{Y|Z} \otimes \mu_Z$.

Hence under the assumptions that $P_{|Z}$ admits a regular version (an assumption also made by [Laumann et al. \(2023\)](#)), the considered random variables operate on compact sets of BV-paths and (16) holds, the test is consistent if and only if $\frac{1}{n} \text{Tr}(PD^{RKHS}) \rightarrow 0$.

B Experiments and Evaluation

This section delves into the experimental framework, elaborating on the data generation process, the parameters and architectures employed, and presents additional results.

B.1 Kernel Heuristic and Interval Choice

In kernel methods, besides selecting the right kernel function, the correct choice of its parameters is vital. A reasonable choice for radially symmetric kernels $k(x_i, x_j) = f(\|x_i - x_j\|/\sigma)$, $f: \mathbb{R}_+ \rightarrow \mathbb{R}_+$ is to choose σ to lie in the same order of magnitude as the pairwise distances $(\|x_i - x_j\|)_{i,j}$. Choosing the bandwidth for the RBF kernel in our setting with samples $(x_i)_{i \in [n]}$, $x_i \in \mathcal{C}^0(I, \mathbb{R}^d)$ is not straight forward, as the RBF kernel ultimately acts on signatures and there is no immediate way in obtaining a ‘typical scale’ of pairwise distances of signatures. To still set the bandwidth purely based on observed data, there are two natural ways to implement a median heuristic based on two different collections of pairwise distances. The first option is to choose

$$\sigma_1 = \text{Median}\{\|x_i - x_j\|_{L^2} \mid i, j \in [n]\},$$

where $\|\cdot\|_{L^2}$ is the L^2 norm of entire paths, i.e., integrated over the time interval I . Given that in practice we observe the paths x_i still at fixed time points $t_1 < \dots < t_m$ within the interval I , we can also consider the heuristic

$$\sigma_2 = \text{Median}\{\|x_{i,t_l} - x_{j,t_k}\|_2 \mid i, j \in [n], l, k \in [m]\},$$

Table 4: Performance of *future-extended h-locally conditionally independence criterion* in the bivariate setting for the two heuristic σ_1 and σ_2 for different sample sizes. The SHD is measured for different values of s in $\mathbb{L}_{s,t}^+$ with $t = 1$, defining different lengths of intervals in the past and future. Overall the performance is best of shorter values of the past intervals compared to the future ($s < \frac{t}{2}$).

$(\times 10^2)$	σ_1		σ_2	
	$n = 400$	$n = 600$	$n = 400$	$n = 600$
$s = 0.1$	76.2 ± 2.5	58.4 ± 2.7	14.9 ± 2.0	15.8 ± 2.0
$s = 0.2$	77.3 ± 2.7	72.2 ± 2.8	12.9 ± 1.7	10.9 ± 1.7
$s = 0.3$	80.2 ± 2.3	76.2 ± 2.6	21.8 ± 2.2	17.8 ± 2.0
$s = 0.4$	89.1 ± 2.0	92.0 ± 2.1	31.7 ± 2.4	25.7 ± 2.2
$s = 0.5$	89.1 ± 2.0	98.1 ± 2.0	38.6 ± 2.5	27.7 ± 2.2
$s = 0.6$	82.4 ± 1.9	96.0 ± 2.1	60.0 ± 2.7	48.5 ± 2.9
$s = 0.7$	102.0 ± 1.2	104.0 ± 2.0	80.2 ± 2.2	61.4 ± 2.7
$s = 0.8$	104.0 ± 1.4	95.0 ± 1.5	81.1 ± 2.0	87.1 ± 2.4
$s = 0.9$	95.0 ± 1.6	104.4 ± 1.8	102.0 ± 1.2	101.0 ± 2.1

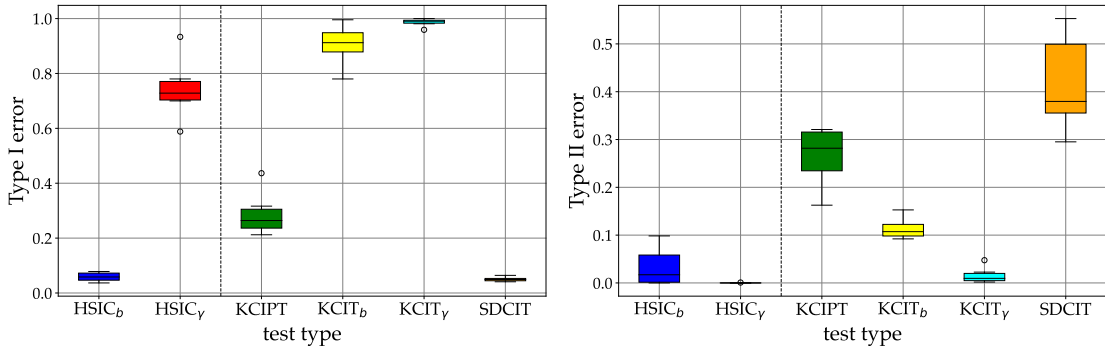


Figure 5: Performance in terms of type I and type II errors of different unconditional (HSIC_b and HSIC_γ) and conditional tests (KCIPT, KCIT_b, KCIT_γ, SDCIT). Among the conditional tests, KCIPT balances type I and type II errors well compared to SDCIT. Among the unconditional tests, HSIC_b outperforms HSIC_γ.

where $\|\cdot\|_2$ is the Euclidean norm in \mathbb{R}^d and we consider pairwise distances of all observations across all paths and time points. In early benchmarks, we have empirically found σ_2 to yield a better heuristic by comparing the performance of both heuristics by evaluation of the SHD in a causal discovery task in the linear bivariate setting $X^1 \rightarrow X^2$ without diffusion interaction with $a_{21} \sim \mathcal{U}((-2.5, -1] \cup [1, 2.5))$, $a_{11}, a_{22} \sim \mathcal{U}((-0.5, 0.5))$ and $\sigma_i \sim \mathcal{U}([0, 0.5))$ (see 4). The experiment is performed for different choices of intervals $[0, s], [s, s + h]$ in the future-extended h -local conditional independence. As can be seen from 4, σ_2 and $[0, 0.1], [0.1, 1]$ seem to perform best on average and are therefore used in the rest of the experiments.

B.2 Empirical Comparison of Different Tests

Different kernel-based conditional and unconditional tests are compared. HSIC with bootstrap (HSIC_b) and with γ -distribution approximation (HSIC_γ) (Gretton et al., 2007) were implemented for the unconditional setting, while KCIPT (Doran et al., 2014), KCIT with bootstrap (KCIT_b), KCIT with γ approximation (KCIT_γ) (Zhang et al., 2011) and SDCIT for the conditional setting (Lee and Honavar, 2017). Figure 5 shows that KCIPT and HSIC_b are overall the best performing ones in terms of type I and type II error.

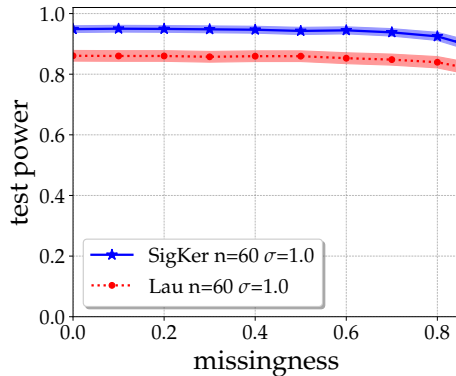


Figure 6: Test power over the missingness level (percentage of observations that is being dropped at random). While both our method as well as [Laumann et al. \(2023\)](#) maintain their power up to high levels of missingness, our test still consistently outperforms the baseline. Lines show means over 1000 settings in Section 4.1 and shaded regions show standard errors.

B.3 Simulated Datasets

The data-generating process corresponding to Table 4 consists in linear Stochastic Differential Equations (SDEs) as defined in Equation 5. The drift matrix elements are created using a uniform distribution, with a_{11} and a_{22} following $\mathcal{U}[-0.5, 0.5]$. The off-diagonal elements, a_{21} and a_{12} , are sampled from $\mathcal{U}[-2.5, -1.0) \cup (1.0, 2.5]$. Additionally, we set both drift and diffusion biases by sampling b_i and d_i from $\mathcal{U}[-0.1, 0.1]$ and $\mathcal{U}[-0.2, 0.2]$, respectively. It’s also important to note that the diffusion matrix in these simulations contains only zero elements.

B.4 Additional Experimental Results for the Bivariate Case

Figure 6 shows that in the simple unconditional bivariate setting of Section 4.1 our test maintains high power up to substantial levels of missingness and only starts degrading once more than 80% of observations are dropped at random starting from 64 time steps over the interval $[0, 1]$ for 1000 different SDEs.

B.5 Building blocks for causal discovery

Similarly to the results in Table 4, we perform the same experiments for the setting in which the causal dependency only comes from the diffusion. Specifically, referring to the linear SDE in eq. (5), $a_{ij} = a_{ji} = 0$, $a_{11}, a_{22} \sim \mathcal{U}[-0.5, 0.5]$, $\sigma_{12}, \sigma_{21} \sim \mathcal{U}[-2.5, -1.0) \cup (1.0, 2.5]$ and $\sigma_{11}, \sigma_{22} \sim \mathcal{U}[-0.5, 0.5]$. Moreover, b_i and d_i are sampled from $\mathcal{U}[-0.1, 0.1]$ and $\mathcal{U}[-0.2, 0.2]$. Table 5 includes the results for all the different causal structures. We also assess the performance of the *future-extended h-locally conditionally independence criterion* ($\perp_{s,t}^+$) in the different three-dimensional causal structures: chain, collider and fork. The results are presented respectively in Table 6. The tables show that the test is able to reconstruct the presence and the directionality of the edges overall all building blocks of causal structure learning.

B.6 Real-World Pairs Trading Example

In the pairs trading experiment, stock price data is downloaded from Yahoo Finance for a predefined list of stocks over a specific period, divided into training (1st January 2010 to 31st December 2011) and trading intervals (1st January 2012 to 31st December 2012). The chose stocks are Trinity Industries (TRN), Brandywine Realty Trust (BDN), Commercial Metals Company (CMC), The New York Times Company (NYT), New York Community Bancorp (NYCB), The Wendy’s Company (WEN), CNX Resources Corporation (CNX). Logarithms

Table 5: Test performance on the key building blocks for causal discovery. Here, $\perp\!\!\!\perp$ refers to $\perp\!\!\!\perp_{\text{sym}}$ except for $X_p^1 \perp\!\!\!\perp X_f^1$ which means $X_{[0,t/2]}^1 \perp\!\!\!\perp X_{[t/2,t]}^1$ in a setting where the dependency only comes from the diffusion. We use KCIPT for CI tests and bootstrapped HSIC unconditional independence. We simulate 40 samples of 512 trajectories for 10 different SDEs (400 tests per column) with 25% of the 128 original observations dropped uniformly at random. The **error** represent type I or type II error when the null hypothesis H_0 should be rejected (\times) or accepted (\checkmark), respectively.

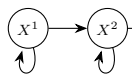
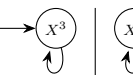
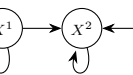
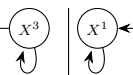
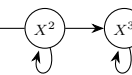
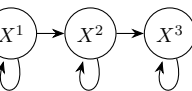
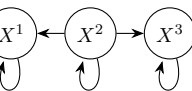
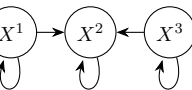
graph								
H_0	$X^1 \perp\!\!\!\perp X^2 X^3$	$X^1 \perp\!\!\!\perp X^3 X^2$	$X^1 \perp\!\!\!\perp X^2 X^3$	$X^1 \perp\!\!\!\perp X^3 X^2$	$X^1 \perp\!\!\!\perp X^3 X^2$	$X_p^1 \perp\!\!\!\perp X_f^1$	$X^1 \perp\!\!\!\perp X^2$	$X^1 \perp\!\!\!\perp X^2$
should reject	\checkmark	\times	\checkmark	\checkmark	\times	\checkmark	\times	\checkmark
error	0.33	0.05	0.11	0.35	0.11	0.00	0.07	0.01

Table 6: Test performance on the chain, fork and collider causal structures for the *future-extended h-locally conditionally independence criterion*. Here, $\perp\!\!\!\perp$ refers to $\perp\!\!\!\perp_{s,h}^+$ and we use KCIPT. We simulate 10 samples of 512 trajectories for 10 different SDEs (100 tests per column). The **error** represent type I or type II error when the null hypothesis H_0 should be rejected (\times) or accepted (\checkmark), respectively.

graph							
H_0	$X^1 \perp\!\!\!\perp X^2 X^3$	$X^2 \perp\!\!\!\perp X^1 X^3$	$X^1 \perp\!\!\!\perp X^3 X^2$	$X^3 \perp\!\!\!\perp X^1 X^2$	$X^2 \perp\!\!\!\perp X^3 X^1$	$X^3 \perp\!\!\!\perp X^2 X^1$	
should reject	\times	\checkmark	\times	\times	\times	\checkmark	
error	0.07	0.33	0.04	0.04	0.03	0.00	
graph							
H_0	$X^1 \perp\!\!\!\perp X^2 X^3$	$X^2 \perp\!\!\!\perp X^1 X^3$	$X^1 \perp\!\!\!\perp X^3 X^2$	$X^3 \perp\!\!\!\perp X^1 X^2$	$X^2 \perp\!\!\!\perp X^3 X^1$	$X^3 \perp\!\!\!\perp X^2 X^1$	
should reject	\checkmark	\times	\times	\times	\times	\checkmark	
error	0.21	0.08	0.06	0.16	0.08	0.30	
graph							
H_0	$X^1 \perp\!\!\!\perp X^2 X^3$	$X^2 \perp\!\!\!\perp X^1 X^3$	$X^1 \perp\!\!\!\perp X^3 X^2$	$X^3 \perp\!\!\!\perp X^1 X^2$	$X^2 \perp\!\!\!\perp X^3 X^1$	$X^3 \perp\!\!\!\perp X^2 X^1$	
should reject	\times	\checkmark	\checkmark	\checkmark	\checkmark	\times	
error	0.10	0.00	0.36	0.46	0.00	0.08	

of the stock prices are computed to stabilize variance and normalize the prices. During the training period, pairs of stocks are selected based on various statistical tests: Cointegration Test (Engle-Granger) to determine if a pair of stocks is cointegrated, suggesting a long-term equilibrium relationship; Augmented Dickey-Fuller (ADF) Test to assess the stationarity of the spread (ratio) of a pair’s prices; and Granger Causality Test to check if the price of one stock in the pair can predict the price of the other. Pairs are selected based on the p-values from these tests, with a threshold of 0.05 determining significance. In the trading phase, a rolling window is used to continuously recalculate the mean and standard deviation of the spread between the selected pairs. Trades are initiated based on the z-score of the spread, where a high z-score indicates a short position and a low z-score indicates a long position. Positions are managed and closed when the spread returns to a predefined z-score threshold. The strategy’s performance is evaluated based on total return, annual percentage rate (APR), Sharpe ratio, maximum drawdown (maxDD), and maximum drawdown duration (maxDDD).

B.7 Evaluation Metrics

Following common conventions in the causal discovery literature, we evaluate our algorithms using the following metrics.

Structural Hamming Distance (SHD) Given two directed graphs $\mathcal{G}_1 = (V, \mathcal{E}_1)$, $\mathcal{G}_2 = (V, \mathcal{E}_2)$ over the same nodes with different sets of edges and let $A_1, A_2 \in \{0, 1\}^{n \times n}$ be their adjacency matrices. Then we define the structural hamming distance (SHD) as

$$\text{SHD} = \sum_{i,j \in [n]} |(A_1)_{ij} - (A_2)_{ij}|$$

Normalized SHD In order to compare the recovery performance of our algorithms for different types of graph-sizes, the normalized SHD is defined as

$$\text{SHD}_{\text{norm}} = \frac{\text{SHD}}{d(d-1)}$$

C Baselines

In the experiment section Section 4, we benchmark our method against other baselines, including Granger causality, CCM, PCMCI, and Laumann (Laumann et al., 2023). For the latter, we used their implementation provided in the `causal-fda` package. For the Granger-implementation for two variables ($d = 2$), we used Seabold and Perktold (2010), for CCM we used Javier (2021), and for PCMCI we used the `tigramite` package (Runge et al., 2019). In PCMCI, tests for edges are conducted by applying distance correlation-based independence tests (Székely et al., 2007) between the variables’ residuals after regressing out other nodes using Gaussian processes.

D Summary of notations

A summary of notation is provided in Table 7.

E Extension to the Cyclic Setting

Given that we are considering the dynamic setting, it is generally natural to allow for \mathcal{G} to have cycles. This comes at no additional requirement of consistency constraints as it does in the static case (see for example Bongers et al. (2021)), since the causal arrows in the model eq. (1) should be thought of as ‘pointing towards the infinitesimal future, with infinitesimal

Table 7: Summary of notations

Symbol	Meaning
d	total number of components in stochastic process $X = (X^1, \dots, X^d)$ / nodes in graph
n_k	dimension of the k-th component X^k
m_k	dimension of the k-th Brownian motion W^k
n	total dimension of the stochastic process X with $n = n_1 + \dots + n_d$
$T \in \mathbb{R}_{>0}$	maximum observation time
$t, s \in [0, T]$	some arbitrary time points
$\mathcal{G} = (V, \mathcal{E})$	directed graph \mathcal{G} with nodes V and edges \mathcal{E}
$[m]$	short for $\{1, \dots, m\}$

magnitude', integrated over the whole time interval considered. Indeed, the system of SDEs does not require any global consistency to be well-posed, other than the regularity and growth conditions that guarantee global-in-time existence and uniqueness.